END
DATE
FILMED
9 83
DTIC

		4.5	2.8		2.5
	1.0	5.0			
		5.6	3.2		2.2
			3.6		
	1.1		4.0		2.0
					1.8
	1.25		1.4		1.6

MICROCOPY RESOLUTION TEST CHART

NATIONAL BUREAU OF STANDARDS - 1963 - A

ADA131881
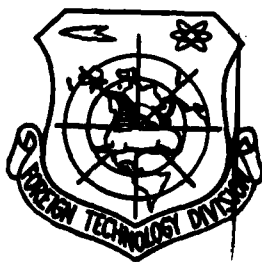
FOREIGN TECHNOLOGY DIVISION

JOURNAL OF THE CHINESE SOCIETY OF ASTRONAUTICS

(Selected Articles)

S DTIC
ELECTE
AUG 29 1983 D

D

DTIC FILE COPY

83 08 25 179

FTD -ID(RS)T-0898-83

EDITED TRANSLATION

FTD -ID(RS)T-0898-83   Date 21 Jul 19 83

Table of Contents

i

GRAPHICS DISCLAIMER

All figures, graphics, tables, equations, etc. merged into this
translation were extracted from the best quality copy available.

ii

THE ANALYSIS FOR THE REGULATION PERFORMANCE OF A VARIABLE
THRUST ROCKET ENGINE CONTROL SYSTEM

by Zhou Xiwen

Abstract

This paper introduces the constituent, operation principle
and regulation process of the bipropellant variable thrust
rocket engine for a variable area injector that uses solenoid
valve control.

According to the constituent and practical operation process
of an engine control system, the mathematical models of each link
is given and the transfer function method is used to analyze the
dynamic and steady performances of engine control systems. The
use of concrete numerical calculations further shows the major
factors influencing the dynamic performance and steady errors for
the engine control system.

I. The Constituent and Operation Principle of Engine Control
   Systems

This paper will introduce the use of a control circuit which
possesses a certain operating frequency and changeable pulse
width to control two high performance solenoid valves. The use
of the flow quantity change of liquids to change the pressure of
the injector's hydraulic pressure chamber will cause the up and
down movements of the injector's needle valve to change the area
of the flow, control the flow quantity of the propellant and
realize thrust changes. The control system is mainly composed of
a control circuit, solenoid valve and thrust chamber with a var-
iable area injector. Fig. 1 shows the relationship between them.
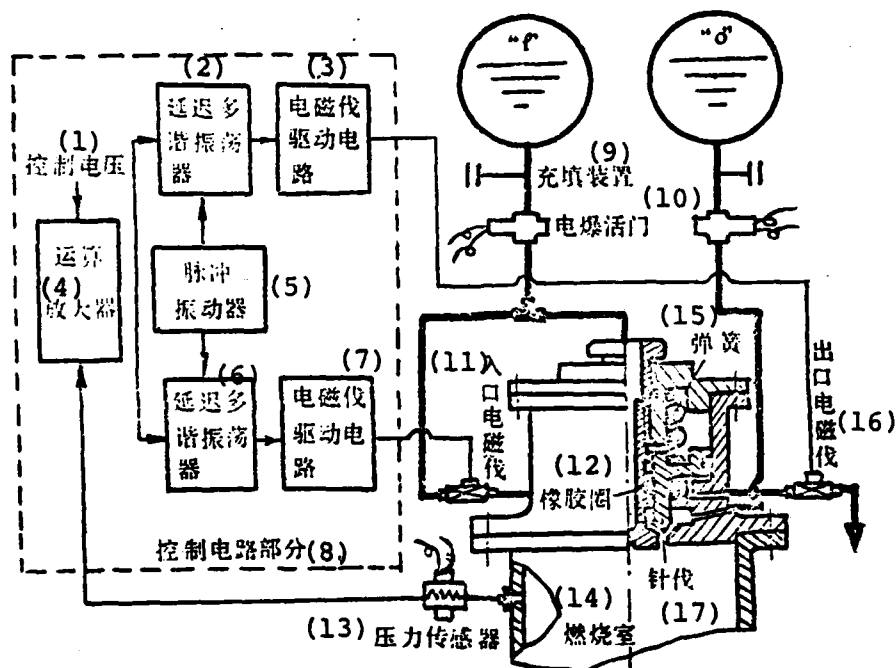
Fig. 1   Systems chart of the operation principle of the engine.
Key: (1) Control voltage; (2) Delay multivibrator;
(3) Solenoid valve drive circuit; (4) Operational
amplifier; (5) Pulse vibrator; (6) Delay multivibrator;
(7) Solenoid valve drive circuit; (8) Control circuit
section; (9) Filling device; (10) Electric explosion
valve; (11) Entrance solenoid valve; (12) Rubber ring;
(13) Pressure sensor; (14) Combustion chamber; (15)
Spring; (16) Exit solenoid valve; (17) Needle valve.

The control circuit is composed of an operational amplifier,
pulse vibrator, delay multivibrator and solenoid valve drive
circuit etc. The operational amplifier carries out superposition
operations of the control circuit signals as well as the combus-
tion chamber's feedback signals and supplies voltage error
signals. The pulse vibrator gives voltage pulse signals with
certain frequency and amplitude and controls the delay multivi-
brator. The delay multivibrator controls the pulse operation of
changing width based on the frequency of the pulse vibrator and
size of the operational amplifier's output voltage error. These
pulse signals which possess certain frequency width variations

2

are amplified by the solenoid valve drive circuit and drive the solenoid valve pulses.

The two solenoid valves are connected to the injector's hydraulic pressure cavity. When the error signals of the control circuit are positive voltage signals, the control entrance solenoid valve operates, the pressure of the hydraulic pressure cavity rises, the needle valve of the thrust injector lifts up, the nozzle area of the injector enlarges, the flow of the propellant increases and the thrust rises. On the other hand, when the error signals of the control circuit are negative voltage signals, the control exit solenoid valve operates and eliminates the liquid in the hydraulic pressure cavity causing the pressure in the hydraulic pressure cavity to decrease. When the injector's needle valve is under the effects of the spring force, the flow area of the nozzle decreases, the flow of the propellant decreases and the thrust also decreases.

The control working substance of the injector's needle valve uses a propellant which is passed through the entrance solenoid valve into the hydraulic pressure cavity. Because the flow of the control fluid is very small, it passes through the exit solenoid valve and is directly discharged into the atmosphere. We can also design a system wherein the control fluid returns again to the incendiary agent's main pipeline.
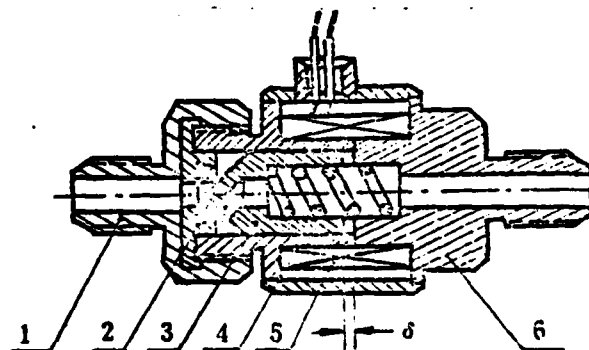
Fig. 2

Fig. 2   Diagram of the structure of the solenoid valve.
Key: (1) Exit connecting nozzle; (2) Needle valve seat;
(3) Needle valve; (4) Spring; (5) Coil; (6) Entrance
connecting nozzle.

We can see from the above that this type of variable thrust
rocket engine system uses the change of the size of the injector's
flow area to change the flow of the propellant and attain thrust
regulation.   The propellant supply system of the engine does not
carry out regulation.   The special features of its plan are that
the control system is simple, operation is reliable but regula-
tion precision is not sufficiently high.
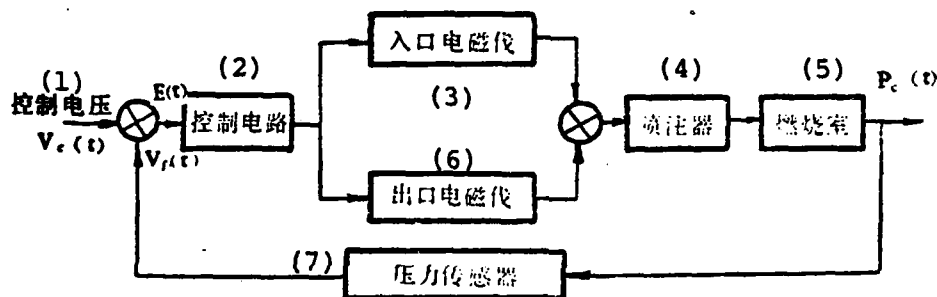
Fig. 3   Block diagram of the control system.
Key: (1) Control voltage; (2) Control circuit;
(3) Entrance solenoid valve; (4) Injector; (5) Combustion
chamber; (6) Exit solenoid valve; (7) Pressure sensor.

The operating parameters of the control circuit are as
follows:

Source voltage of the control circuit   V=28   [V]

Control voltage of the circuit V_c=0 ~ 5   [V]

Operating frequency of the pulse oscillating circuit
  f=50 ~ 100 [H_z]

Output voltage of the feedback pressure sensor
  V_f=0 ~ 5   [V]

Output voltage of the operational amplifier
  V_A=0.1 ~ 1.1 ~ 2.1   [V]

4

II. Mathematical Equations of the Main Links of the Control System

The solenoid valve of the engine control system is controlled by the control circuit and carries out variable width pulse operations. Therefore, we establish mathematical models for the control circuit and solenoid valve. During mathematical process ing, the Laplace transformation of the non-continuous system will be encountered, that is, the problem of the Z transformation.

However, the control system's input signals - control voltage V_c and output signal - thrust chamber pressure p_c are continuous signals and only the intermediate links are pulse signals. In order to simplify the overelaborate mathematical deductions, we establish mathematical models for the main links such as the circuit, solenoid valve, injector, combustion chamber etc. based on the practical operation and regulation state of the engine system as well as the processing of the continuous system:

1. The Control Circuit Equation Basic Hypotheses:

1) The pulse operating frequency of the control circuit is fixed. The size of the circuit's operating frequency influences the dynamic and steady state performances of the engine system. Moreover, the size of the frequency is also influenced by the performance of the solenoid valve itself. Tests show that the operating frequency of the engine system which we introduced can be selected within the range of 50 $\sim$ 1,000 H_z.

2) The pulse width of the control circuit forms a direct ratio with the voltage deviation (the difference between the control voltage and feedback voltage - the deviation signal). (Tests prove that the pulse width and voltage deviation basically change within a direct ratio).

In order to raise the dynamic and steady state performances

5

of the engine system, the pulse width should be regulated as
wide as possible. The pulse frequency of the control circuit
and the pulse width do not influence eachother and they can be
separately regulated.

3) The leading edge starting time of the solenoid valve is
fixed. Because the solenoid valve is an inductive unit, the
electromagnetic force must overcome the fictional force, spring
force, damping force and hydraulic pressure etc. of the needle
valve. The electromagnetic force is in direct ratio with the
size of the electric current and the change of the electric cur-
rent with the time rises according to the exponential curve and
thus forms the leading edge when the solenoid valve opens. The
operating electric current curve of the solenoid valve is shown
in Fig. 4. Starting leading edge τ_e=3 ~ 5ms, the opening time
of the needle valve τ_f=0.5ms and τ_b is called the effective
pulse width of one pulse of the solenoid valve.
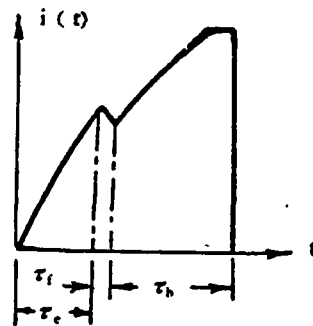

Fig. 4 Operating electric current curve of the solenoid valve.

Based on the above analysis, we can give the circuit -
solenoid valve equation.

$$K_b = \frac{\tau_b}{E_o} \qquad (1)$$

In the formula, K_b is the circuit gain [S/V], $E_o = V_c - V_f$ is
the difference between the control voltage and feedback voltage
[V], when V_f=0 then $E_o - V_c$ and τ_b is the effective pulse

6

width [S].

After the engine is regulated to the operating state and the pulse frequency is selected, the pulse width is regulated to its maximum width and K_b is also fixed.

For example, $f = 50 H_z$, $E_o = V_c = 5V$ corresponds to the maximum pulse width and when $\tau_e + \tau_b = 20ms$ ($\tau_e = 5ms$, $\tau_b = 15ms$, τ_f is deleted), then $K_b = \tau_b / E_o = 3 \times 10^{-3}$ [S/V].

The pulse width equation of the solenoid valve is

$$b(t) = K_b \cdot E(t) \qquad (2)$$

In the unit time of the solenoid valve there is a effective operating time called the solenoid valve effective pu operating coefficient. It is indicated by η (t). Naturally,

$$\eta(t) = f b(t) \qquad (3)$$

In the formula, f is the pulse operating frequency $[H_z]$ of the solenoid valve and η (t) is the effective pulse operating coefficient (η (t) $<$ 1).

2. The Solenoid Valve's Flow Equation

Basic hypotheses:
1) After the solenoid valve passes leading edge time τ_e within a pulse operating time, the needle valve instantaneously opens.

Due to the fact that after the solenoid valve passes leading edge time $\tau_e = 3 \sim 5ms$ the time that the needle valve is open is only $\tau_f = 0.5ms$, $\tau_f \lll \tau_b$, therefore τ_f can be deleted.

2) Tests prove that when the closing time - trailing edge of the solenoid valve's needle valve is smaller than 0.5ms, it can be deleted and it can be considered that the needle valve is

7

instantaneously closed.

Based on the above hypotheses, when considering the structural measurements of the solenoid valve, we can arrange the flow equation of the entrance solenoid valve and exit solenoid valve.

The flow equation of the entrance solenoid valve is:

$$Q_1'(t) = \mu A \sqrt{\frac{2g}{\gamma}[p_o - p_H(t)]}$$

In the formula, μ is the flow coefficient and A is the flow area [mm^2] of the solenoid valve which is calculated from the geometric dimensions of the solenoid valve (see reference [2]):

$$A = 2.22\delta(D -)/2)$$

δ is the maximum interval [mm] of the solenoid valve's open needle valve:

$$\delta \approx 0.1 \sim 0.4 mm$$

D is the diameter [mm] of the solenoid valve's exit, P_o is the fluid pressure [kg/mm^2] and $P_H(t)$ is the hydraulic pressure cavity's pressure [kg/mm^2] of the thrust chamber's head.

The exit solenoid valve's flow equation is:

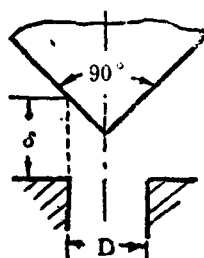$$Q_2'(t) = \mu A \sqrt{\frac{2g}{\gamma}P_H(t)}$$

Fig. 5 Geometric measurements of the solenoid valve.

The fluid of the exit solenoid valve directly discharges into the atmosphere.

The solenoid valve is pulse operated and because of this the practical flow of the solenoid valve should introduce the effective pulse operating coefficient $\eta(t)$. Therefore, the flow equations of the entrance solenoid valve and exit solenoid valve are:

$$Q_1(t) = \eta(t)\mu A \sqrt{\frac{2g}{\gamma}[P_0 - P_H(t)]}$$

$$Q_2(t) = \eta(t)\mu A \sqrt{\frac{2g}{\gamma}P_H(t)}$$

We substitute the $\eta(t)$ and b(t) of equations (2) and (3) into the above equation and let

$$K_0 = fK_b\mu A \sqrt{\frac{2g}{\gamma}} \qquad (4)$$

Then, the above flow equation becomes:

$$Q_1(t) = K_0 E(t)\sqrt{P_0 - P_H(t)}$$
$$Q_2(t) = K_0 E(t)\sqrt{P_H(t)}$$

We know from the operating principle of the engine system mentioned above that when the deviation of the control voltage and feedfack voltage is $E(t) > 0$, the control entrance solenoid valve operates. On the contrary, when $E(t) < 0$, the exit solenoid valve operates, that is, when the two solenoid valves operate, which one operates depends on whether the deviation signal E(t) is positive or negative.

In order to use one equation in the control circuit to indicate the solenoid valve's flow equation, it is necessary to employ two functions. Letting:

$$u(e) = \frac{1}{2|E(t)|}[|E(t)| + E(t)] \qquad (5)$$

$$v(e) = \frac{1}{2|E(t)|}[|E(t)| - E(t)] \qquad (6)$$

9

Naturally,

$$E(t) > 0, \quad u(e)=1, \quad v(e)=0;$$

$$E(t) < 0, \quad u(e)=0, \quad v(e)=1.$$

and then the solenoid valves' flow equations are:

$$Q_1(t) = K_Q u(e) E(t) \sqrt{P_o - P_H(t)} \tag{7}$$

$$Q_2(t) = K_{Qv}(e) E(t) \sqrt{P_H(t)} \tag{8}$$

These are binary nonlinear equations and based on the design requirements used for the engine, the regulation amplitude of each thrust is relatively small and the regulation changes of the thrust are transitionally smooth. We can use the Taylor series to linearize the two equations. For the entrance solenoid valves it is:

$$Q_1(t) = \frac{\partial Q_1(t)}{\partial E(t)}\bigg|_{t} E(t) - \frac{\partial Q_1(t)}{\partial P_H(t)}\bigg|_{t} \Delta P_H(t).$$

In the formula:

$$\frac{\partial Q_1(t)}{\partial E(t)}\bigg|_{t} = K_Q u(e)\sqrt{P_o - P_{Ht}} = K_Q K_i'$$

$$\frac{\partial Q_1(t)}{\partial P_H(t)}\bigg|_{t} = K_Q \frac{1}{2} u(e) E_t [\sqrt{P_o - P_{Ht}}]^{-1} = K_Q K_i''$$

Within this,

$$K_i' = u(e)\sqrt{P_o - P_{Ht}} \tag{9}$$

$$K_i'' = \frac{1}{2} u(e) E_t [\sqrt{P_o - P_{Ht}}]^{-1} \tag{10}$$

Letting

$$K_u' = K_Q K_i' \tag{11}$$

$$K_u'' = K_Q K_i'' \tag{12}$$

then

$$Q_1(t) = K_u' E(t) - K_u'' \Delta P_H(t) \tag{13}$$

We obtain the flow equation of the exit solenoid valve in the same way:

$$Q_2(t) = K_i' E(t) + K_i'' \Delta P_H(t) \tag{14}$$

10

In the formula:

$$K'_u = K_0 K'_u \qquad (15)$$

$$K''_u = K_0 K''_0 \qquad (16)$$

$$K'_0 = v(e)\sqrt{P_{Hi}} \qquad (17)$$

$$K''_0 = \frac{1}{2} v(e) E_i [\sqrt{P_{Hi}}]^{-1} \qquad (18)$$

Equations (13) and (14) are indicated by one equation:

$$Q(t) - Q_1(t) - Q_2(t) - (K'_u - K'_v) E(t) - (K''_u + K''_v) \Delta P_H(t)$$

Letting

$$K_e = K'_u - K'_v$$

$$K_{PH} = K''_u + K''_v$$

then

$$Q(t) = K_e E(t) - K_{P_H} \Delta P_H(t) \qquad (19)$$

Naturally, when $E(t) > 0$, $K_e = K'_u$, $K_{P_H} = K''_u$, $Q(t) = Q_1(t)$; $E(t) < 0$, $K_e = K'_v$, $K_{P_H} = K''_v$, $Q(t) = -Q_2(t)$.

The Laplace transformation formula corresponding to the flow equation of the solenoid valve is:

$$Q(s) = K_e E(s) - K_{PH} P_H(s) \qquad (20)$$

3. Equation of the Thrust Chamber Head's Containing Chamber

When the pressure of the thrust chamber head's containing chamber, based on design requirements $P_H(t) < 20 kg/cm^2$, is compared with the common hydraulic system, the containing chamber's pressure is lower. In the containing chamber equation, it is not necessary to consider the containing chamber case and the deformation of the air caused by the pressure in the containing chamber.
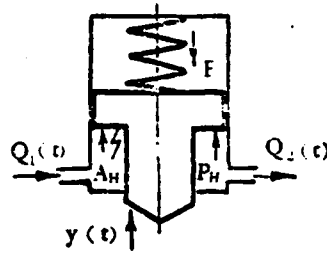
Fig. 6. The hydraulic containing chamber.

Because the spring has prestress F_0, when $F_0 = A_H P_H$, the injector's needle valve opens and moves, that is, when $P_H(t) = P_{H_0}$, $y(t) = 0$. Therefore,

$$A_H dy(t) = Q(t) dt$$

When $dy(t) > 0$, $Q(t) = Q_1(t)$; when $dy(t) < 0$, $Q(t) = Q_2(t)$.

$$y(t) = \frac{1}{A_H} \int Q(t) dt \tag{21}$$

The corresponding Laplace transformation formula is:

$$Y(s) = \frac{1}{A_H} \cdot \frac{1}{S} Q(s) \tag{22}$$

4. The Equation of the Injector;s Needle Valve Movement

Fig. 7 shows the stress conditions of the injector's needle valve.
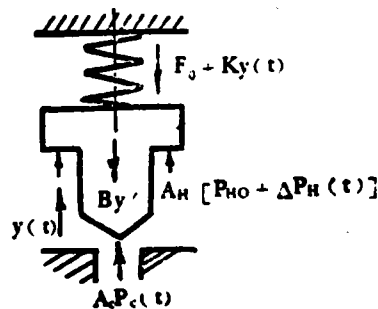
Fig. 7 Stress chart of the injector's valve.

12

F_o	is the spring's prestress [kg]
K	is the spring's rigidity [kg/mm]
$y(t)$	is the needle valve's displacement [mm]
$dy(t)/dt$	is a certain moment's movement speed of the needle valve [mm/s]
P_{H_o}	is the hydraulic pressure when the needle valve begins to rise [kg/mm^2]
$\triangle P_H(t)$	is the increment of the hydraulic pressure [kg/mm^2]
A_H	is the operating area of the hydraulic pressure [mm^2]
B	is the damping coefficient of the needle valve's movement [kg·s/mm]
A_C	is the operating area of the gas towards the needle valve [mm]
$P_C(t)$	is the gas pressure [kg/mm^2]
m	is the needle valve's mass [kg·s^2/mm]

The equation injector needle valve's movement is (see reference [1]):

$$m \frac{d^2 y(t)}{dt^2} + B \frac{dy(t)}{dt} + Ky(t) = A_C P_C(t) + A_H \triangle P_H(t) \qquad (23)$$

The corresponding Laplace transformation formula is:

$$(mS^2 + BS + K) Y(s) = A_C P_C(s) + A_H P_H(s) \qquad (24)$$

5. The Equation of the Injector's Flow

$$G_o(t) = \mu_o A_o \sqrt{2g \gamma_o \triangle P_o} \qquad \text{oxidizing agent}$$

$$G_f(t) = \mu_f A_f \quad 2g \gamma_f \quad P_f \qquad \text{incendiary agent}$$

Many tests have proven that when the displacement of the injector's needle valve is relatively small, the changes of the flow and displacement form a linear relationship. The two flow equations can be expressed as:

$$G_o(t) = \gamma_o y(t) \qquad (25)$$

$$G_f(t) = \gamma_f y(t) \qquad (26)$$

13

In the formula, coefficients γ_o and γ_f can be determined by flow tests of the injector.

The corresponding Laplace transformation formula of the flow equation is:

$$G_o(S) = \gamma_o Y(S) \qquad (27)$$
$$G_f(S) = \gamma_f Y(S) \qquad (28)$$

6. The Combustion Chamber Equation

Basic hypotheses:

1) Combination delay τ is constant and it is considered that passing τ time after the propellant is sprayed into the combustion chamber, the gas is instantaneously produced.

2) The gas is an ideal gas.

3) When comparing the flow changing speed and pressure wave propagation speed, it is consiered that the pressure wave propagation speed is infinitely great and the pressure of the combustion chamber at each location is uniform at any given moment.

We can obtain the combustion chamber equation (see reference [1]) based on the above hypotheses.

$$\frac{V_c}{RT_s} \frac{dP_c(t)}{dt} + \frac{A_t}{\beta} P_c(t) = G_o(t-\tau) + G_f(t-\tau) \qquad (29)$$

In the formula,

V_c is the volume of the combustion chamber $[mm^3]$

R is the constant of the ideal gas $[mm/°K]$

T_c is the gas temperature $[°K]$

A_t is the area of the nozzle throat $[mm^2]$

β is the comprehensive parameter of the combustion chamber $[s]$

14

The corresponding Laplace transformation formula is:

$$\frac{v_c}{RT_c}S+\frac{A_t}{\beta} \quad P_c(s)=e^{-\tau s}[G_o(s)+G_f(s)] \tag{30}$$

7. The Equation of the Feedback Pressure Sensor and Circuit
Operational Amplifier

The pressure sensor used for this engine system is a resist-
ance type pressure sensor. We can consider that it is an
amplification link for this type of sensor. Its equation is:

$$V_f(t)=K_f P_c(t) \tag{31}$$

The circuit operational amplifier equation is:

$$E(t)=V_c(t)-V_f(t) \tag{32}$$

The corresponding Laplace transformation formulas are:

$$V_f(s)=K_f P_c(s) \tag{33}$$

$$E(s)=V_c(s)-V_f(s) \tag{34}$$

III. The Transfer Function of the Engine Control System

We synthesize formulas (20), (22), (24), (27), (28), (30),
(33) and (34) and use a block diagram to indicate the relationship
between each variable.

Fig. 8 Block diagram of the control system.

15
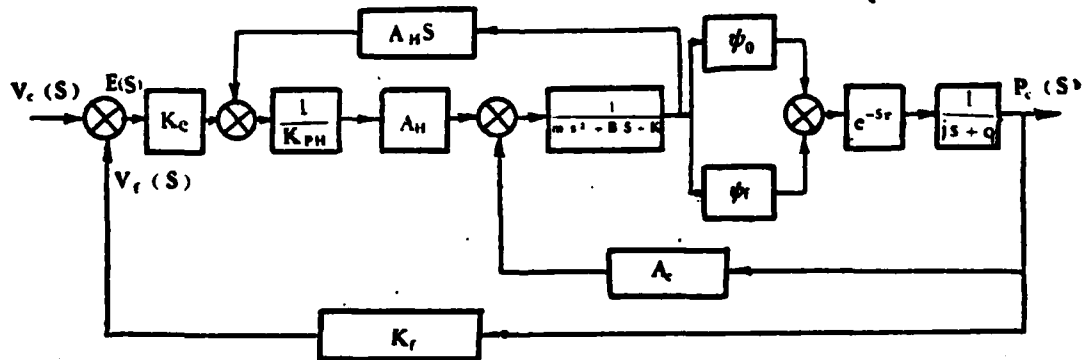
In the diagram, $j = v_c/RT_c$, $q = A_t/\beta$.

Because the engine uses a bipropellant natural propellant, ignition delay time τ is relatively small. Generally, $\tau < 5ms$ which can be considered $e^{-s\tau} = 1$.

Volume v_c of small engine combustion chambers is relatively small, temperature T_c of the gas is relatively high and $RT_c \gg v_c$. It can be considered that $j = v_c/RT_c = 0$.

The block diagram is simplified into the following form:

$$W(s) = \frac{K_e K_c A_H/K_{P_H}}{ms^2 + (B + A_H^2/K_{P_H})S + K - K_c A_c} \tag{35}$$

In the formula

$$K_c = \frac{1}{q}(\gamma_0 + \gamma_f) = \frac{\beta}{A_t}(\gamma_0 + \gamma_f) \tag{36}$$

K_c is called the combustion chamber's gain [kg/mm^3].
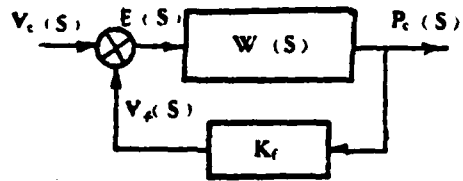
Fig. 9 Block diagram of simplification.

The closed-cycle transfer function of the control system is:

$$\phi(s) = \frac{K_e K_c A_H/K_{P_H}}{ms^2 + (B + A_H^2/K_{P_H})s + K - K_c A_c + K_c K_c K_f A_H/K_{P_H}} \tag{37}$$

m   is the mass of the injector's needle valve [kg·s^2/mm]

B   is the damping coefficient of the injector's needle valve [kg·s/mm]

A_H is the operating area of the needle valve [mm^2]

16

K_{P_H} is the solenoid valve's pressure coefficient [$mm^5/s \cdot kg$]

K_e is the solenoid valve's flow gain [$mm^3/s \cdot V$]

K is the spring's rigidity [kg/mm]

K_c is the combustion chamber's gain [kg/mm^3]

A_c is the operating area of the needle valve's gas [mm^3]

K_f is the gain of the feedback pressure sensor [mm^2V/kg]

When calculating the transfer function, the B, P_{Ht} (when t=0, $P_{Ht}=P_{H0}$) and K_c can be determined by the test method based on the concrete structure and operating parameters of the engine.

IV. Analysis of the Performance of the Engine Control System

1. Analysis of the Stability of the Control System

The characteristic equation of the control system's transfer function is:

$$mS^2 + (B + A_H^2/K_{P_H})S + K - K_cA_c + K_eK_cK_fA_H/K_{P_H} = 0$$

Letting

$$\lambda = B + A_H^2/K_{P_H}, \quad \nu = K - K_cA_c + K_eK_cK_fA_H/K_{P_H}$$

The root of the characteristic equation is:

$$S_1 = \frac{-\lambda + \sqrt{\lambda^2 - 4m\nu}}{2m} \tag{38}$$

$$S_2 = \frac{-\lambda - \sqrt{\lambda^2 - 4m\nu}}{2m} \tag{39}$$

Because $\lambda > 0$, to discuss the stability of the control system it is only necessary to discuss root S_1 of the characteristic equation. We can see from root S_1 of the characteristic equation that:

1) When $\nu < 0$, then we have the real root of $S_1 > 0$, the output's transition component has monotonic increases based on the

17

exponential law and the system is unstable. However, even if the plan of this engine control system appears unstable, the combustion chamber's pressure will not be able to have monotonic increases or decreases. Because the control system is a closed-cycle system with feedback, when the combustion chamber's pressure exceeds a certain value, this can cause the corresponding solenoid valve to operate. This type of combustion chamber pressure can operate according to certain frequency and amplitude oscillation mode. The exit and entrance solenoid valves operate alternately.

2) When the real root of $v > 0$, $\lambda^2 - 4mv > 0$ and $S_1 < 0$ and the control system is stable.

3) When $v > 0$, $\lambda^2 - 4mv < 0$, S_1 and S_2 are the conjugate complex roots of the characteristic equation and the transition component of the output function appears as an oscillation mode.

In order to further display that these parameters are major influencing factors of the dynamic state performance of the engine control system, we used the parameters of the engine to carry out concrete calculations.

Original parameters:

(1) 名　　称	(2) 符　号	(3) 单　　位	(4) 数　　值
(5) 喷注器针阀质量	m	$kg \cdot s^2/mm$	1.2×10^{-6}
(6) 针阀液压作用面积	A_H	mm^2	16×10^1
(7) 针阀燃气作用面积	A_e	mm^2	2.5×10^1
(8) 针阀阻尼系数	B	$kg \cdot s/mm$	3.6
(9) 弹簧刚度	K	kg/mm	120

(10) 名　　称	(11)符　号	(12)单　　位	(13)数　　值
(14) 电磁阀流通面积	A	mm^2	0.84
(15) 电磁阀流量系数	μ		0.60
(16) 喷注器针阀液压力	P_{Hi}	kg/mm^2	8×10^{-1}
(17) 电磁阀入口压力	P_e	kg/mm^2	18×10^{-1}
(18) 电路脉冲工作频率	f	Hz	80
(19) 脉冲宽宽	τ_b	S	6×10^{-3}
(20) 电路增益	K_b	S/V	1.2×10^{-1}
(21) 偏差信号电压	E_i	V	2
(22) 压力传感器增益	K_l	$V \cdot mm^2/kg$	55.56

Table 1

Key: (1) Name; (2) Symbol; (3) Unit; (4) Numerical
value; (5) Mass of the injector's needle valve;
(6) Operating area of the needle valve's hydraulic
pressure; (7) Operating area of the needle valve's gas;
(8) Damping coefficient of the needle valve; (9) Rigid-
ity of the spring; (10) Name; (11) Symbol; (12) Unit;
(13) Numerical value; (14) Flow area of the solenoid
valve; (15) Flow coefficient of the solenoid valve;
(16) Hydraulic pressure of the injector's needle valve;
(17) Entrance pressure of the solenoid valve; (18) The
circuit pulse's operating frequency; (19) Pulse width;
(20) Circuit gain; (21) Voltage of the deviation signal;
(22) Gain of the pressure sensor.

During cold tests, we used water as the hydraulic pressure
working substance. We can calculate situations with rising
thrust based on the data given in Table 1:

$$K_0 = f K_b \mu A \sqrt{\frac{2g}{\gamma}} = 6.78 \times 10^3 [mm^4/s \cdot V \cdot kg^{1/2}]$$

$$K_i' = \sqrt{p_e - P_{Hi}} = 0.32 [kg/mm^2]^{1/2}$$

$$K_i'' = \frac{1}{2} E_i [\sqrt{p_e - P_{Hi}}]^{-1} = 0.32 [V \cdot mm/kg^{1/2}]$$

$$K_e = K_0 K_i'' = 2.17 \times 10^3 [mm^3/s \cdot V]$$

$$K_{P_H} = K_0 K_i' = 2.17 \times 10^3 [mm^5/s.kg]$$

If the injector is designed well, when needle valve displacement $h_{max} < 0.25mm$, the change of the injector's flow and needle valve's displacement is close to a linear relationship. The combustion chamber's gain K_c can be expressed as:

$$K_c = \frac{Pc_{max}}{h_{max}}$$

If $Pc_{max} = 10 \times 10^{-2} kg/mm^2$ and $h_{max} = 0.25mm$, then $K_c = 0.40 \ kg/mm^3$.

We can calculate the v and n values in the characteristic equation based on the above mentioned parameters and determine the stability of the engine control system. Moreover, we can also see the influence of each parameter on the transfer function and further analyze the major influencing factors on the dynamic state performance of the engine control system.

$$\nu = K - K_c A_c + K_c K_e K_f A_H / K_{P_H} = 120 - 100 + 355.58 \times 10^2 = 35.578 \times 10^3 \, kg/mm$$

$$\lambda = B + A_H^2 / K_{P_H} = 3.6 + 11.797 \times 10^2 = 11.83 \times 10^2 \, kg \cdot s/mm$$

$$\lambda^2 - 4m\nu = 139.9489 \times 10^4 - 1.71 = 139.487 \times 10^4 (kg \cdot s/mm)^2$$

Calculations show that when $v > 0$ and $n^2 - 4mv > 0$, the root of the transfer function characteristic equation is a negative real root. Therefore, the engine control system is stable.

2. Analysis of the Transition Time of the Engine Control System

Because the mass of the engine injector's needle valve is very small, when $m \ll B + A_H^2 / K_{P_H}$, we can delete the second degree term. The combustion chamber pressure changes measured by heat tests have monotonic rises and decreases based on the exponential curve. Therefore, the engine control system can be simplified into a first order system and the transfer function of equation (37) changes into:

$$\phi(s) = \frac{K_{\circ}K_{\circ}A_{H}/K_{P_{H}} \cdot v}{(\lambda/v)S + 1} = \frac{5}{TS + 1}$$

$5 = K_{\circ}K_{\circ}A_{H}/K_{P_{H}} \cdot v$ （称为放大系数） (1)

$T = \lambda/v$ （称为时间常数） (2)

Key: (1) Called the amplification coefficient;
(2) Called the time constant.

Based on analysis of the first order link, when combustion chamber pressure p_c reaches to 95% of the specified value, its transition time $t_p = 3T$ and therefore:

$$t_p = \frac{3(B + A_H^2/K_{P_H})}{K - K_c A_c + K_e K_c K_f A_H/K_{P_H}} \tag{40}$$

Because the range of change of each parameter is not large, we can see from the previous numerical calculations that:

$$B \ll A_H^2/K_{P_H}, \quad |K - K_c A_c| \ll K_e K_c K_f A_H/K_{P_H}$$

Relational formula (43) of transition time t_p can be simplified into:

$$t_p = \frac{3A_H}{K_e K_c K_f} \tag{41}$$

We can see from formula (41) that the transition time is mainly determined by the injector needle valve's hydraulic pressure operating area A_H and the solenoid valve's flow gain K_e.

In order to reduce transition time t_p, we reduce as much as possible the injector needle valve's hydraulic pressure operating area A_H, appropriately enlarge the solenoid valve's flow area A, increase the pulse width or raise the pulse operating frequency. All of these are effective measures for reducing the transition time.

3. Analysis of the Steady State Errors of the Engine System

21

We can obtain the Laplace transformation expression of deviation signal E(t) from the block diagram in Fig. 9 of the engine control system:

$$E(s) = \frac{1}{1+W(s)K_f} V_c(s)$$

In the formula

$$W(s) = \frac{K_e K_c A_H / K_{P_H}}{ms^2 + (B + A_H^2 / K_{P_H}) S + K - K_c A_c}$$

Control voltage $V_c(t)$ of the engine control system introduced in this article uses the jump function form for input. Therefore, we will only discuss the positional errors of the jump input signals here but we will not discuss the speed errors and acceleration errors.

$$V_c(s) = \frac{K_v}{s}$$

In the formula, K_v is the amplification coefficient of the control voltage [V].

We can obtain the general expression of the steady state error by using the last value theorem of the Laplace transformation.

$$1(t) = \lim_{s \to o} SE(s) = \frac{K_v}{1+W(0)K_f}$$

By substituting in W(0), we can obtain the steady state error expression of the engine control system:

$$l(t) = \frac{K - K_c A_c}{K - K_c A_c + K_e K_c K_f A_H / K_{P_H}}$$

In the same way, $|K - K_c A_c| \ll K_e K_c K_f A_H / K_{P_H}$.

The steady state error expression can be simplified into the following form:

22

$$l(t) = \frac{K - K_c A_c}{K_e K_c K_f A_H / K_{P_H}} K_v$$

From formulas (9), (10), (11) and (12), we obtain:

$$\frac{K_e}{K_{P_H}} = \frac{2}{E_t} (p_o - P_{Ht})$$

Then, the steady state error expression is:

$$l(t) = \frac{(K - K_c A_c) E_t}{2 K_c K_f A_H (p_o - P_{Ht})} K_v \tag{42}$$

Enlargement of spring rigidity K and reduction of the injector needle valve's hydraulic pressure operating area A_H can cause steady state error $l(t)$ to increase.

When the regulation range of the thrust is large and deviation signal E_t is large, then the steady state error is large. The steady state errors are larger when there is high thrust (P_{Ht} is large) regulation than when there is low thrust (P_{Ht} is small) regulation.

The situations discussed above are concerned with rising thrust. As for situations with descending thrust, the solenoid valve's flow gair K and the solenoid valve's pressure coefficient K_{P_H} are substituted into relational formulas (15), (16), (17) and (18), that is, by using the exit solenoid valve's parameters and other invariant parameters, we can obtain the same analytical results.

We should also point out that in the analysis of the regulation performance of the engine control system, we did not take into consideration the steady state errors of the components of the engine control system which are caused by the structural parametric

changes which influence their sensitivity. For example, when
the interval of the solenoid valve's needle valve movements
enlarge, the magnetic resistance enlarges and the leading edge
of the open needle valve enlarges, these cause the steady state
errors to increase. In the same way, when the solenoid valve's
entrance pressure p_o enlarges and the starting force increases,
this can also cause the leading edge of the open needle valve to
enlarge and influence the dynamic and steady state performances.
Furthermore, the nonlinearity etc. of the feedback pressure
sensor can also influence the regulation performance of the
engine control system but these factors were not included in the
above analysis.

References

[1] The Basis of the Linear Theory for the Regulation of Liquid
    Rocket Engines, The No. 103 Teaching and Research Section
    of the Changsha Engineering College, 1977.

[2] The Design of Solenoid Valves for Liquid Rocket Engines,
    The No. 103 Teaching and Research Section of the Changsha
    Engineering College, 1977.

[3] J.J. Rodden, R.J. Pollak, "Servo Control of a Variable
    Thrust Rocket," ARS Journal, 1960.10.

[4] 50 Pound Thrust Attitude Control Motors, AD 411336.

ELECTRONIC SERVO VALVE
by Cai Yongnian

Abstract

This paper presents a new type of electronic servo valve
(ESV) which is composed of a pulse modulator, electro-mechanical
actuator and variable section area valves. The operating prin-
ciple and transfer function for ESV are also described. At the
same time, we also give test data on ESV.

I. Introduction

ESV are composed of servo circuits made up of integrated
circuits, motors and variable section area valves. The feedback
effects of mounting a position sensor on a valve rod causes this
type of valve to have relatively high static precision and
relatively fast actuation time. With the use of millivolt or
volt level command voltage, it can control the flow of the medium
within a very wide range. The relationship between the command
voltage and flow can be linear and it can also be nonlinear. The
servo circuit is installed in a case. The motor and variable
section area valve combine into an organic whole. The servo
circuit is connected by the cable and motor. The entire structure
of the ESV is shown in Fig. 1.

Fig. 1 Entire structure of the ESV.

25

Because this type of valve does not require a supplementary air source and hydraulic source in the process of controlling the flow, this type of valve is especially applicable in situations which do not have an air source and hydraulic source. At the same time, this valve is also applicable for control of poisonous mediums and situations which do not allow people to work. Therefore, this valve possesses relatively strong structural adaptability.

One of the specific applications of the ESV is its use to change the thrust of a spacecraft's liquid rocket engine so as to cause the spacecraft to be able to complete soft landing, variable orbit flight and other complex space navigation tasks on planets. Figs. (2), (3) and (4) show the situations of the actual test runs. Fig. 2 is the situation when the thrust is relatively large and because of this the corresponding flame is relatively long. Figs. (3) and (4) are the situations when the thrust is intermediate and relatively small and because of this the corresponding flames are relatively short. In Figs. (2), (3) and (4), the upper part of the combustion chamber has two similar ESV. One controls the oxident of the engine and one controls the fuel of the engine.

P-675997 P-675998

P-675999

图(2) 图(3)
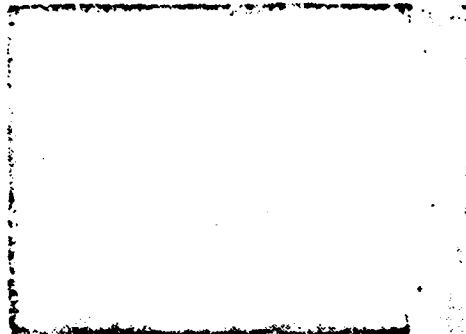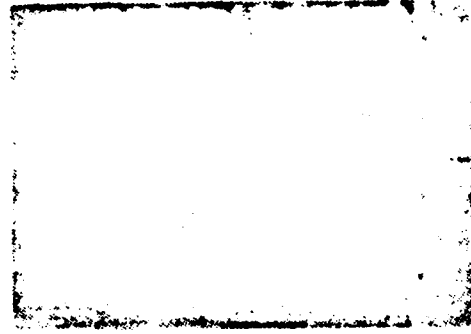
Figs. 2, 3 and 4.

II. Fundamental Principle

The ESV is composed of a servo circuit, motor and variable section area valves. The position sensor is installed on the end of t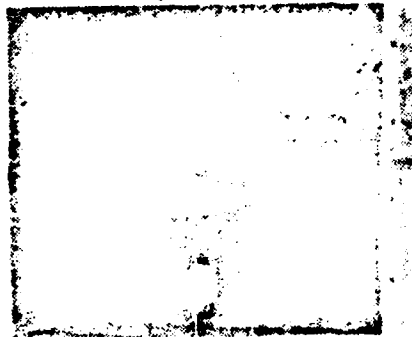he valve rod and uses the feedback effects of the position sensor to cause this type of valve to have general closed-cycle system performance.
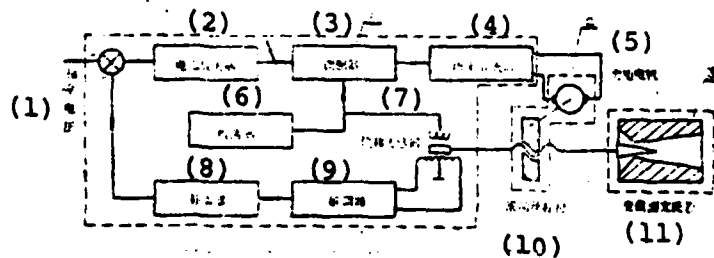

Fig. 5 Chart of the principle of the ESV system.
(see next page for key)

27

Fig. 5

Key: (1) Command voltage; (2) Voltage amplifier;
(3) Modulator; (4) Power amplifier; (5) Torque motor;
(6) Oscillator; (7) Displacement sensor; (8) Compen-
sator; (9) Demodulator; (10) Rolling lead screw;
(11) Variable section area venturi.

Dotted line frame 1 in Fig. 5 is the servo circuit. It
includes the voltage comparator, modulator, power amplifier,
oscillator, demodulator, compensator etc. The major function of
the servo circuit is to amplify the very weak error signals and
transform them into pulse modulated width signals which can drive
the motor. The frequency of the pulse is determined by the fre-
quency of the oscillator. The width of the pulse is determined
by the size of the error signal. The voltage amplifier, modula-
tor and power amplifier are positive loops of the closed-cycle
system. The demodulator and compensator are feedback loops of
the closed-cycle system. Broken line frame 2 in Fig. 5 is the
motor's final control element. It is composed of the permanent
magnet type torque motor and the rolling lead screw. The lead
screw transforms the rotating movement of the motor's roll into
the direct movements of the valve rod. The guide bar of the
displacement sensor is fastened on the end of the valve rod. The
output voltage of the displacement sensor is the input signals of
the demodulator. Broken line frame 3 of Fig. 5 is the variable
section area valve. It can be the variable section area venturi
and can also be the variable section area current-limiting ring.
The movable valve rod extends into the opening of the venturi or
current-limiting ring. The valve rod is machined into a certain
taper in the throat area near the venturi and the smallest aper-
ture of the current-limiting ring. Because of the effect of
this tapering, when the valve rod moves to the left and right,
this causes the flow area to have corresponding changes which
changes the flow quantity. Structurally, the motor and valve
sections are joined by the mechanical method. Figs. (6) and (7)
are detailed blueprints of this type of structure.

28
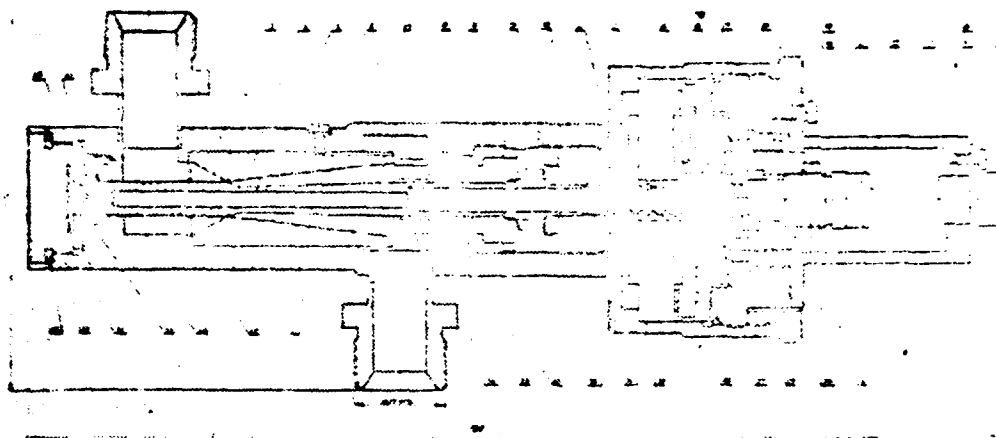
Fig. 6 Full diagram of the motor mechanism and variable section area venturi.
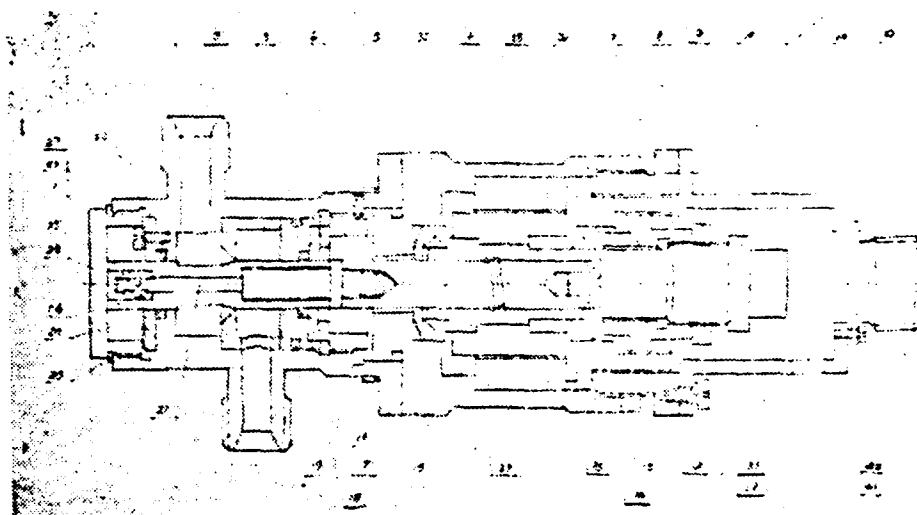
Fig. 7 Full diagram of the motor and the variable section area current-limiting ring.

The structure in Fig. 6 uses the venturi to control the flow quantity. The structure in Fig. 7 uses the current-limiting ring to control the flow quantity. The structures of the two are basically the same, only the structures of the valve sections are different. The external dimensions of Fig. 7 are smaller than those of Fig. 6.

The operating principle of the ESV is as follows. When the system is in a holding state, the error signal in front of the voltage amplifier is zero (in reality, it is not zero but very small). Therefore, after passing the modulator and power amplifier, the pulse signals added to the torque motor are pulse signals with equal widths. Because the mean value of the pulse signals with equal widths is zero, the torque motor does not rotate. Therefore, the valve rod is also in the static state. At this time, the output signals of the displacement sensor are zero. When the command mechanism gives a certain command voltage because the output signals of the displacment sensor are zero, error signals are produced. The error signals are amplified and modulated by the positive loop which causes the error signals to change into corresponding pulse signals with unequal widths. Because the mean voltage of the pulse signals with unequal widths is zero, the motor rotates. The rolling lead screw rotates and changes the movements of the motor into direct movement of the valve rod. Following the movement of the valve rod, the displacement sensor then gives the corresponding electric signals. With the effects of the feedback loop, these electric signals are transformed into corresponding position feedback signals and they are compared to the command voltage. After comparison, the obtained error signals are again regulated according to the above mentioned process. When the regulation process is completed, the error signals are zero, the valve rod stops moving and each position of the valve rod corresponds to each command voltage. The relationship between them is zero.

III. The Transfer Function of the ESV

Because the response time of an electronic package is much faster than that of the motor and valve, when the time constant of the electronic package is omitted, we simplify Fig. 5 into Fig. 8. We deduce its transfer function based on Fig. 8
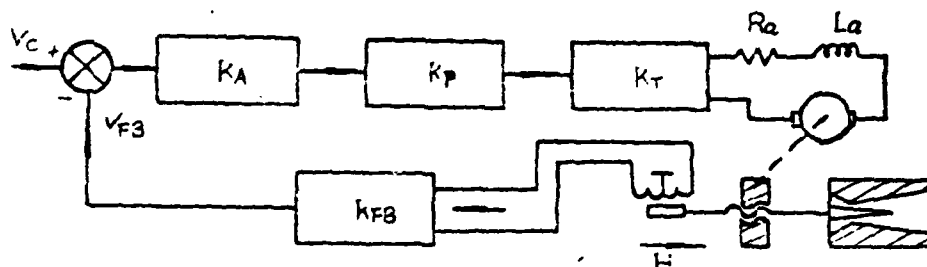
Fig. 8. Block diagram of the ESV.

We can see from Fig. 8 that the terminal voltage of the two terminals of the motor's armature can be expressed by the following formula:

$$E_a = (V_c - V_{F3})K_A K_P$$

The differential equation of the armature circuit is as follows:

$$E_a = L_a \frac{di}{dt} + R_a i_a + e_b$$

Torque T produced when the armature was under a corresponding speed is in direct ratio to the armature's electric current. Its relational formula is as follows:

$$T = K_T i_a$$

Counter electromotive force e_b in the armature loop can be expressed by the following formula:

$$e_b = K_b \frac{d\theta}{dt}$$

The armature rotates at a corresponding speed. At the same time, the produced torque will satisfy Newton's second law. The obtained equation is as follows:

$$T = J \frac{d^2\theta}{dt^2} + f \frac{d\theta}{dt} + T_c + T_L$$

The transfer effect of the lead screw causes the friction coefficient of the valve section converted on the motor's axis to change very little. Thus, the f in the above formula is actually the viscous friction coefficient of the motor's axis.

31

T_c is the friction torque converted on the motor's axis caused by the dynamic seal of the two terminals of the valve rod.

(When) 当 $\dfrac{d\theta}{dt} > 0$时 $T_c = + M_c$

(When) 当 $\dfrac{d\theta}{dt} < 0$时 $T_c = - M_c$

M_c in the above formula is the friction torque caused by the coulomb friction. T_L is the load torque of the fluid hydraulic power converted on the motor's axis. The transfer effect of the rolling lead screw causes the driving torque in the aforementioned formula to be $T \gg T_c + T_L$. In order to simplify the calculation and analysis of the simplified system, we omitted the effects of $T_c + T_L$. In this way, we caused the nonlinear differential equation to be simplified into a linear differential equation. Its formula is as follows:

$$T = J\,\dfrac{d^2\theta}{dt^2} + f\,\dfrac{d\theta}{dt}$$

Drawing support from the drive effects of the lead screw, the rotating movements of the motor's armature change into linear movements of the valve rod. Its relational formula is:

$$\dfrac{1}{2\pi}\,\theta = H$$

After Laplace transformation and arrangement, the block diagram after the Laplace transformation is as shown in Fig. 9 and the transfer function corresponding to it is as follows:

$$\dfrac{H(S)}{V_c(S)} = \dfrac{K_A K_P K_T \dfrac{1}{2\pi}}{S[L_a J S^2 + (L_a f + R_a J)S + R_a f + K_T K_b] + K_A K_P K_T K_{FB} \dfrac{1}{2\pi}}$$
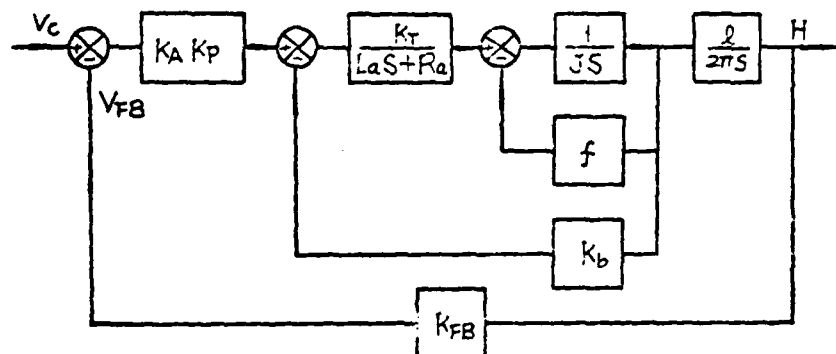
Fig. 9 Block diagram of the Laplace transformation of the ESV.

The root locus of the above as yet uncompensated transfer function is shown in Fig. 10. After K_{FB} and $\frac{1}{2\pi}$ are selected, when K_A, K_P and K_T are relatively low, the system indicated by the root locus chart is stable. However, when K_A, K_P and K_T become very large, the system is unstable which was proven by tests.
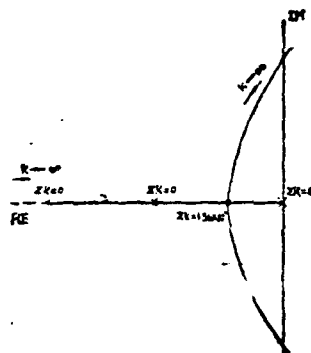
Fig. 10 Root locus chart of the ESV.

IV. Selection of the Unit

The comparison amplifier is the convergent area of the command signals, position feedback signals and compensating signals. Its reliability and stability will directly influence the performance of the system. The polarity of the command signals and the polarity of the feedback signals are opposite when the frequency is relatively low. The compensating signals are used to improve the

33

performance of the system. The above mentioned comparator amplifier uses a common solid state unit - the operational amplifier. See Fig. 11 for its principle. Its output voltage V_o can be indicated by the following expression:

$$V_\bullet = -\left[V_C \frac{R_F}{R_1} - V_{FB} \frac{R_F}{R_2} - V_{com} \frac{R_F}{R_3}\right].$$
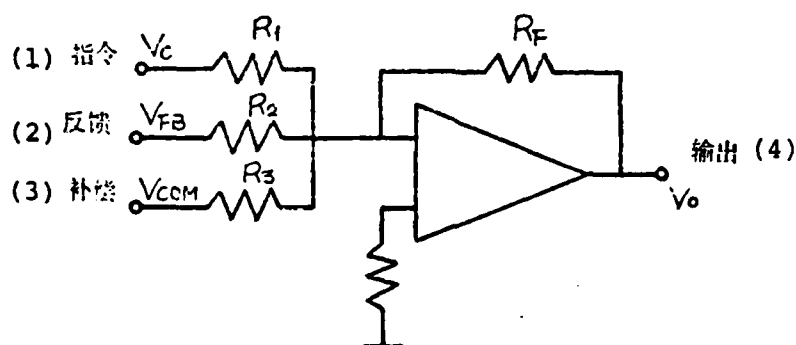
Fig. 11 Chart of the principle of the voltage comparator.
Key: (1) Command; (2) Feedback; (3) Compensator; (4) Output.

In the figure, R_1, R_2 and R_3 are isolation resistances. When $R_1 = R_2 = R_3$, then the above formula changes to:

$$V_o = [V_{FB} + V_{CO_m} - V_c] \frac{R_F}{R_1}$$

The comparison amplifier amplifies the error signals and afterwards sends them to the modulator. The modulator transforms the error signals into equally high pulse signals. The modulator also uses the common operational amplifier. The input terminal of the modulator is the sum total of the error signals and triangular waves. Use of the high gain and limiting effects of the operational amplifier causes the input signals of the modulator to transform into equally high rectangular pulses with

34

variable widths. The chart of its principle is shown in Figs. (12) and (13).
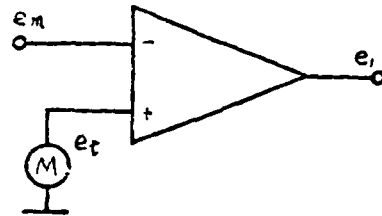
Fig. 12 Chart of the principle of the modulator.
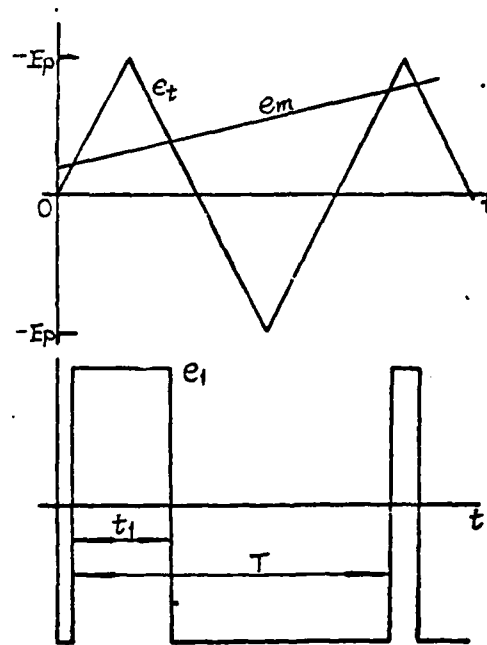
Fig. 13 Chart of the waveforms of the modulator.

If e_m is the output voltage of the comparison amplifier, e_t is the triangular wave's voltage, the triangular wave peak-peak voltage amplitude is $\pm E_p$ and the void ratio occupied by the modulator's output pulses in R, then R can be expressed as follows:

$$R+0.5- \frac{e_m}{2E_p} = \frac{t_1}{T}$$

In the formula, T is the pulse period and t_1 is the width of

35

the modulated pulse. In order to obtain the linear relationship between R and e_m, the linearity of the triangular waves must be very good.

The power amplifier of the driving motor uses a switching amplifier. The output power of this type of circuit can be very large yet the generated heat of the output power tube is very small. Its principle is shown in Fig. 14.
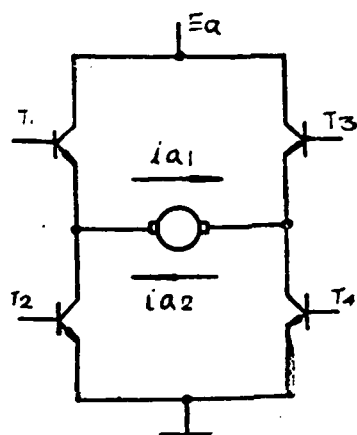
Fig. 14 Chart of the principle of the switching amplifier.

Its operating principle is: when the T_1 and T_4 are conducting, the armature's current is the i_{a1} shown in Fig. 14. When the T_3 and T_4 power tubes are conducting, the current is i_{a2}. Therefore, when the conducting time of the power tubes is changed, this can cause the motor to have positive and negative rotation. In one pulse period, the voltage of the two ends of the armature is E_a in the t_1 time interval. In the $T-t_1$ time interval, the voltage of the two ends of the armature is $-E_a$. Because of this, within one pulse period, the differential equation of the armature circuit can be expressed as follows:

$$L_a \frac{di_a}{dt} + i_a R_a + e_b = E_a \qquad 0 \leqslant t \leqslant t.$$

$$L_a \frac{di_a}{dt} + i_a R_a + e_b = -E_a \qquad t_1 \leqslant t \leqslant T$$

It is well known that the current solution of the above equation is exponentially shaped. Therefore, comparison is complex. In order to simplify the solution of the equation, let us first consider the e_b item. The steady state formula of e_b is:

$$e_b = K_b 2\pi n$$

In the formula, K_b is the reaction coefficient of the armature which is determined by the structure of the motor and n is the rotating speed of the armature. In order to bring the advantages of the torque motor into full play, its operating state should approach the blocked rotating point and also rotate at very low rotating speeds. In order to satisfy the 100 millisecond time interval required for the entire process of valve movement, the minimum rotating speed of the motor must be greater than 12 rotations/second. However, the integration time of the afore-mentioned equation's solution of the current (i.e. one pulse period) is very small. The pulse period T selected for this valve is less than 0.5 milliseconds. This time interval is much smaller than the time required for one turn of the armature ($\frac{1}{12}$ second = 83 milliseconds). Therefore, it is reasonable to consider that within the integration time, the rotating speed of the motor is constant and invariant. Thus, it is assumed that e_b does not change within one pulse period. Secondly, in design, we sought to have the armature's resistance R_a be as low as possible. If we used mean current $I_a = \frac{1}{T} \int i_a(t) dt$ to represent i_a, the product of $R_a I_a$ is very small and thus the proportion occupied by it in V_a is also very small. If we use mean voltage V_a to represent the sum of the above two items, then we can approximately consider that $V_a = i_a R_a + e_b = I_a R_a + e_b$ is constant and invariant. The approximate solution of the above obtained cor-responding armature current is shown in the following formula:

$$i_a(t) = i_a(0) + \frac{E_a - V_a}{L_a} t \qquad 0 \leqslant t \leqslant t_1$$

$$i_a(t) = i_a(t_1) - \frac{E_a + V_a}{L_a} - (t - t_1) \qquad t_1 \leqslant t \leqslant T$$

37

The current changes appearing on the two ends of the armature
are indicated by the following formula:

$$\Delta i_a = \frac{E_a T}{2L_a} (1-\rho^2)$$

In the formula, $\rho = \frac{V_C}{V_{Cmax}}$. When $V_C=0$, then $\rho=0$. At this time,
the current changes of the two ends of the armature are maximum
values:

$$i_{amax} = \frac{E_a T}{2L_C}$$

We can see from the above that when the motor does not rotate,
there is an alternating current flowing in the armature. The
generation of heat is not advantageous. Yet, because there are
continuous positive and negative direction currents in the arma-
ture, the armature is as if in a "dynamic lubrication" state.
This type of state is advantageous to restarting the motor.

The displacement sensor is the main sensitive element of the
feedback loop. In order to increase the anti-interference per-
formance of the system, the output signals of the displacement
sensor are detected by the phase demodulating method. Naturally,
increasing the resolution of the displacement sensor's output
signals and decreasing the phase shift of the output signals
will further improve the performance of the valve system.

In order to reduce the action time and lighten the weight of
the mechanical drive, this plan uses the permanent magnet
torque motor to drive the motor. Because this type of motor pos-
sesses low speed and high torque performance, this motor avoids
the use of a decelerator and thus reduces the space. Use of a
combination of this type of torque motor and rolling lead screw
can cause the relatively small rotating moment to transform into
relatively large thrust or pulling force. See the figures in
Fig. 6 and the right half of Fig. 7 for details of the structure.
Number 1 in Fig. 6 is the torque motor, and numbers 7 and   15

38

are rolling lead screws. Number 36 in Fig. 7 is the torque
motor and symbol 37 is the rolling lead screw. The relationship
between thrust F on the lead screw and torque T of the torque
motor is expressed by the following formula:

$$T = \frac{TL}{2\pi} \ (K + \frac{1}{\eta})$$

In the formula, K is the empirical coefficient which commonly
uses 0.1 to 0.2 and L is the spin moment. η is the drive power
and in most situations, $\frac{L}{2\pi} \ (K + \frac{1}{\eta}) \gg 1$. Therefore, $F \gg T$ and
relatively small torque can produce relatively large thrust.

In this system, the variable section area valve has two struct-
ures. One is the variable section area venturi. Its structure can
be seen in Fig. 6. The other is the variable section area current-
limiting ring. Its structure can be seen in Fig. 7. In a certain
position, the valve rods of the two are machined into a certain
taper. In the movement process of the valve rod, due to the
effects of this taper, the circular flow area continually changes.
The effects begin from the surface and control the flow. After
deductions and arrangements, the relational formula of distance H
of the valve rod's movement and controlled flow quantity Q is:

$$Q = \mu \cdot \pi \cdot H \cdot \sin\alpha (D - H \sin\alpha \cos\alpha) \sqrt{2g\gamma(P_1 - P_{os})}$$

The above relational formula is suitable for the variable section
area venturi as well as for the variable section area current-
limiting ring. When it is a variable section area current-
limiting ring, the P_{os} in the above formula should change to
P_2. P_{os} is the fluid's saturated steam pressure. P_2 is the down-
stream pressure of the valve. When half tapered angle a of the
valve rod is relatively small, the Q-H properties of the variable
section area venturi are linear.

V. Tests and Data

This valve underwent water flow tests, medium tests and

39

ignition test runs. The systems chart of the water flow tests
is shown in Fig. 15.
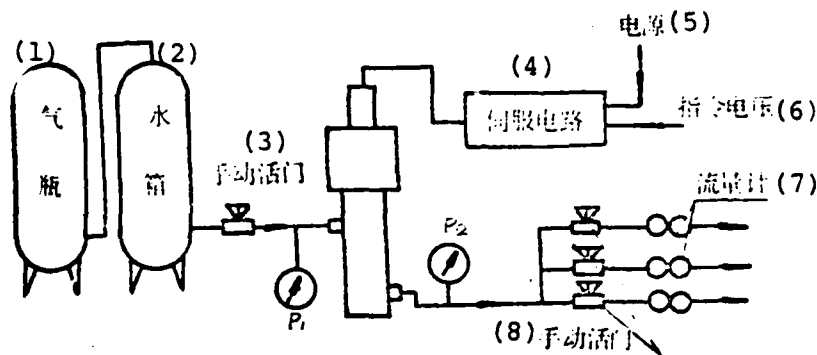
Fig. 15 Systems chart of the water flow tests.

   Key: (1) Air bottle; (2) Water tank; (3) Manual
   operated valve; (4) Servo circuit; (5) Electric
   source; (6) Command voltage; (7) Flow meter;
   (8) Manual operated valve.

The entrance pressure is indicated by P_1. The exit pressure is
indicated by P_2. There are three flow meters in the system's
downstream and their aim is to measure the flow quantity in a
very wide range. Fig. 16 shows the degree of opening character-
istics of the variable section area venturi.
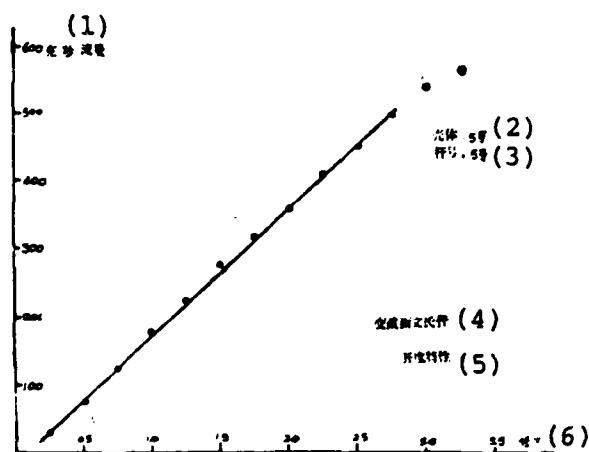
Fig. 16 Opening characteristics of the variable section area
venturi.

   Key: (1) Grams/second, flow; (2) Casing:no. 5; (3) Rod
   number: no. 5; (4) Opening characteristics of the var-
   iable section area venturi; (5) Millimeters.

40

Fig. 17 is the steam corrosion characteristics of the variable section area venturi. The vertical coordinate is the flow quantity and the horizontal coordinate is the reverse voltage of the downstream. The solid lines and points of inflection in the figure are the test values. The broken lines are elongated lines. Each line in the figure corresponds to the degree of opening of the valve. We can see from the curve that the gas corrosion characteristics of this type of venturi increase with the decreases of the degree of opening of the valve.
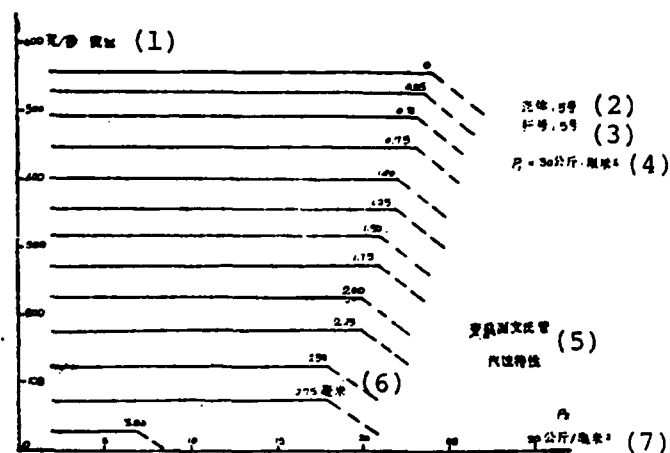
Fig. 17   Gas corrosion characteristics of the variable section area venturi.

Key: (1) Grams/second, flow; (2) Casing: no. 5; (3) Rod number: no. 5; (4) P_1=30 kg/cm^2; (5) Gas corrosion characteristics of the variable section area venturi; (6) Millimeters; (7) Kg/cm^2.

Fig. 18 shows the characteristics of the degree of opening of the variable section area current-limiting ring. The vertical coordinate is the flow quantity and the horizontal coordinate is the command voltage. When comparing the test processes, it should be pointed out that the control precision of the variable section area venturi's flow quantity is relatively high and the pressure decrease of the valve is relatively large; the influence of reverse pressure on the flow quantity of the variable section area current-limiting ring is relatively large and thus

41

fluctuation is very large. However, the pressure decrease of
the valve can be very small.
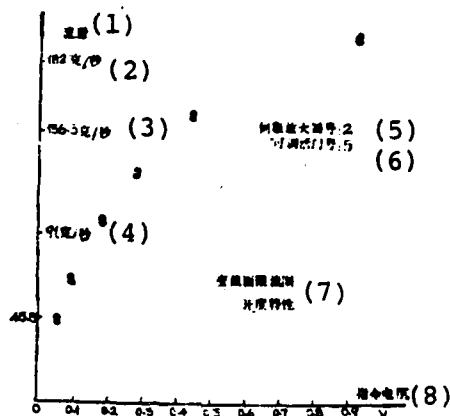
Fig. 18 Characteristics of the degree of opening of the variable
         section area current-limiting ring.

> Key: (1) Flow quantity; (2) Grams second; (3) Grams/
> second; (4) Grams/second; (5) Servo amplifier number:2;
> (6) Adjustable valve number: 5; (7) Characteristics of
> the degree of opening of the variable section area
> current-limiting ring; (8) Command voltage.

VI. Conclusion

     After the first stage of design and production, tests showed
that the ESV could be used to continuously change the flow
quantity of the fluid. By using it we can compose a constant
value automatic regulating system of the flow quantity and a
follow-up system of the flow quantity. After the ESV is added
on to the combustion chamber, we can compose a bipropeller or
single propeller variable thrust engine. Its test conditions can
be seen in Figs. 2, 3 and 4. This valve is also suitable for use
in other situations which require continuous control of the flow
quantity.

Explanation of Symbols Used in This Article

$\overset{\bullet}{V}$ voltage
K   amplification coefficient
R   resistance

42

T   torque, period
t   time variable
L   inductance
J   mechanical inertia
S   Laplace transformation operator
o   half taper angle
u   flow quantity coefficient
Q   flow quantity
P   pressure
Υ specific gravity
g   gravitational acceleration
F   Force

Explanation of Lower Symbols

C   command
FB   feedback
A   amplification
P   power amplification
com compensation
a   armature loop
L   load

References

[1] "Throttleable Thruster System". Final Report. Report No. 70.
     4726. 3-28, JPL Contract 952344.

[2] Shoho Shogan, Modern Control Engineering, Kagaku Shuppansha,
     1976.

[3] David F. Stout, "Handbook of Operational Amplifier Circuit
     Design". McGraw-Hill Book Company (1976)18-9 24-17.

[4] Jacob Tal, "Design and Analysis of Pulsewidth-Modulated
     Amplifier for DC Servo System". IEEE Trans. Vol. IECT-23
     No. 1pp. 47-55.

[5] Mizuho Ninomiya, "Maintaining Ball Screw Precision".
     Machine Design Vol. 51 Number 8 pp. 105-107, April 12, 1979.

THE SELECTION OF LAUNCH TIME FOR NEAR-EARTH SATELLITES (SPACE-CRAFT) WITH MISSION OF VISIBLE PHOTOGRAPH

by Fan Jianfeng

Abstract

This paper presents a set of formulas which can determine the launch time of the visible photographic satellite. If these formulas are applied to determine the launch time, the satellite will have the maximum photographic latitude or a given area will be photographed in a specific time.

I. Preface

When satellites equipped with visible light cameras carry out observation photography of the earth, if the area does not have good light or it is a dark night, then the satellite will be unable to take good photographs or the film will come out blank. This article studies the laws of the spot below the satellite being illuminated by solar light when an observation satellite is taking visible photographs of the earth. Based on these laws, selection of the appropriate launch time can satisfy the various requirements of visible photography. For example, obtaining the maximum photographic area or photographing specified areas at specific local times.

II. The Coordinate System

In selecting the equatorial coordinate system, the position of point B is indicated by right ascension λ and declination φ. The right ascension is measured from Spring equinox point Υ along the equator towards the east, from 0° to 360°. The declination is measured along the equatorial circle, from 0° to ± 90°. From the equator north is positive and towards the south is negative as shown in Fig. 1.

44
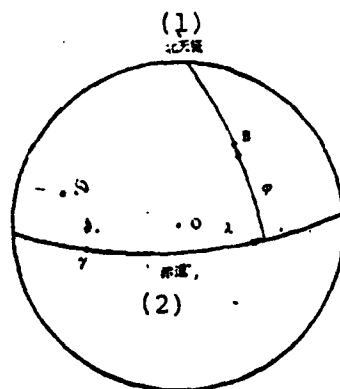
Fig. 1

Key: (1) North pole; (2) Equator.

III. The Photographic Arc

If the right ascension of the sun S is $a_\odot$ and the declination is $\delta_\odot$, then the projection of the demarcating line (not including twilight shadows) of the brightness and darkness of the earth on a celestial sphere is great circle I as shown in Fig. 2.
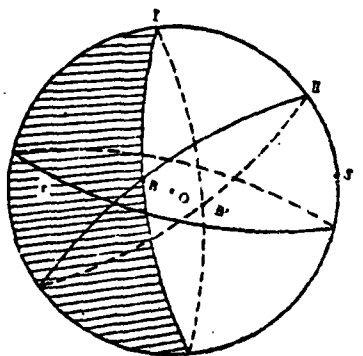

Fig. 2

We call this great circle I the shadow area great circle. Its equation is:

$$-\text{ctg}\,\varphi\,\cos(a_\odot - \lambda) = \text{tg}\,\delta_\odot \qquad (1)$$

If the included angle of the satellite's orbital surface and the surface of the equator is i and the angular distance from Spring equinox point r to ascending node A is Ω, the projection of the satellite's orbit on the celestial body is great circle II as shown in Fig. 2. We call great circle II the orbital great circle. Its equation is:

$$\sin(\lambda - \Omega)\,\text{ctg}\,\varphi = \text{ctg}\,i \qquad (2)$$

In order to determine photographic arc BIIB' (see Fig. 2), we must find the positions of nodes B and B' of great circles I and II. For this reason, we introduce variable Φ and let:

$$\text{tg}\,\Phi = \text{tg}\,\varphi / \cos\lambda$$

Therefore, formulas (1) and (2) can be written as:

$$\frac{\text{tg}\,\lambda}{\text{ctg}\,a_\odot} + \frac{\text{tg}\,\Phi}{\cos a_\odot\,\text{ctg}\,\delta_\odot} = -1 \qquad (1A)$$

and

$$\frac{\text{tg}\,\lambda}{\text{tg}\,\Omega} - \frac{\text{tg}\,\Phi}{\sin\Omega\,\text{tg}\,i} = 1 \qquad (2A)$$

By solving formulas (1A) and (2A), we can obtain:

$$\text{tg}\,\lambda = \frac{\text{tg}\,\delta_\odot\,\text{tg}\,i\sin\Omega - \cos a_\odot}{\text{tg}\,\delta_\odot\,\text{tg}\,i\cos\Omega + \sin a_\odot} \qquad (3A)$$

$$\text{tg}\,\varphi = \pm \frac{\text{tg}\,i\cos(a_\odot - \Omega)}{[1 + \text{tg}^2\,\delta_\odot\,\text{tg}^2\,i + 2\text{tg}\,\delta_\odot\,\text{tg}\,i\sin(a_\odot - \Omega)]^{1/2}} \qquad (3B)$$

Therefore, we obtain the coordinates of nodes B and B' of great circles I and II:

$$\lambda_B = \text{tg}^{-1}\left(\frac{\text{tg}\,\delta_\odot\,\text{tg}\,i\,\sin\Omega - \cos a_\odot}{\text{tg}\,\delta_\odot\,\text{tg}\,i\,\cos\Omega + \sin a_\odot}\right) \qquad (4A)$$

$$\varphi_B = \text{tg}^{-1}\left(\frac{\text{tg}\,i\cos(a_\odot - \Omega)}{[1 + \text{tg}^2\,\delta_\odot\,\text{tg}^2\,i + 2\text{tg}\,\delta_\odot\,\text{tg}\,i\,\sin(a_\odot - \Omega)]^{1/2}}\right) \qquad (4B)$$

$$\lambda_{B'} = 180° + \lambda_B \qquad (4C)$$

$$\varphi_{B'} = -\varphi_B \qquad (4D)$$

46

Solar coordinates $a_\odot$ and $\delta_\odot$ in the above formulas can be looked up in an astronomical calendar. After satellite injectors, orbit inclination can be considered invariant and ascending node angular distance Ω is composed of two parts: initial value Ω_o and the oblateness of the earth perturbation $\Delta\Omega$.

IV. The Relationship of Ω_o and the Launch Time

The injection time of the satellite influences Ω_o and the ascent orbit of the satellite can usually be considered to be given. Therefore, as soon as the launch time is given, the injection time is also determined and thus the launch time influences Ω_o.

If Z is the orbit insertion point, φ_z is the latitude of the orbit insertion point and ψ is the orbit insertion direction (measured from north to east) as shown in Fig. 3.

Fig. 3

From Fig. 3 we can obtain:

$$\Omega_o + \Delta\lambda_z = a_\odot - (12^h - t_z) \tag{5A}$$

In the formula, 12^h represents 12 hours, t_z represents the injection time (local time of the orbit insertion point). In the formula, $\Delta\lambda_z$ has the following relational formula:

$$\mathrm{tg}\,\Delta\lambda_z = \mathrm{tg}\,\psi\,\sin\varphi_z$$

47

Therefore, we can obtain:

$$\Omega_o = a_\theta - 12^h - tg^{-1}(tg\ \psi\ \sin\ \varphi_z) + t_z \qquad (5B)$$

V. Local Time of Each Point on the Photographic Arc

If M is an arbitrary point on the photographic arc and its latitude is φ_M, then we have a formula analogous to formula (5A):

$$\Omega + \Delta\lambda_M = a_\theta - (12^h - t_M)$$

In the formula, t_M is the local time of point M and $\Delta\lambda_M$ has the following relational formula:

$$\sin\Delta\lambda_M = ctgitg\varphi_M$$

Thus, we can obtain:

$$\Omega = a_\theta - 12^h - \sin^{-1}(ctgitg\varphi_M) + t_M$$

By using formula (5B), we finally obtain:

$$t_M = \sin^{-1}(ctgitg\varphi_M) - tg^{-1}(tg\varphi\ \sin\varphi_z) + \Delta\Omega + t_z \qquad (6)$$

Because orbit inclination i only depends on the orbit insertion point's latitude and the orbit insertion direction, we can see from formula (6) that the local time of each point of the photographic arc is related to the injection time, orbit insertion direction and orbit insertion point's latitude. In most situations, the orbit insertion point's latitude and the orbit insertion latitude are often limited by the demands of each area. Thus, if we want to photograph assigned areas in specific local times, we can select an appropriate injection time t_z so that t_M in formula (6) has the desired value.

VI. The Maximum Photographic Area

If satellites with missions of visible photograph are not used to observe specific areas on the ground but carry out common observations of various areas on the ground, then it is hoped

that the satellite can photograph as many ground areas as possible.

1. The Situation of Observation Satellites With Missions of Photograph in Short Flights

Because the photographic film carried by most satellites with missions of photograph is limited, flight time does not exceed several days. Therefore, when analyzing the maximum photographic latitude, we can take $a_\odot$ and $\delta_\odot$ as constants. In this way, we find the derivative of the $\mathrm{tg}\,\varphi_B$ for Ω from formula (3B) and letting the derivative be zero, we can obtain:

$$\sin^2(a_\odot-\Omega)+(\mathrm{tg}\,i\,\mathrm{tg}\,\delta_\odot+\mathrm{ctg}\,i\,\mathrm{ctg}\,\delta_\odot)\sin(a_\odot-\Omega)+1=0$$

By solving the above formula, we obtain:

$$\sin(a_\odot-\Omega)=-\mathrm{tg}\,i\,\mathrm{tg}\,\delta_\odot \qquad (i\leqslant 90°-|\delta_\odot|) \qquad (7A)$$

or

$$\sin(a_\odot-\Omega)=-\mathrm{ctg}\,i\,\mathrm{ctg}\,\delta_\odot \qquad (i\geqslant 90°\,|\delta_\odot|) \qquad (7B)$$

Therefore, there are not many flight days, we can eliminate $\Delta\Omega$, use Ω_0 to replace Ω and obtain:

$$\left.\begin{array}{l} \Omega_{01}=a_\odot-\sin^{-1}(-\mathrm{tg}\,i\,\mathrm{tg}\,\delta_\odot) \\ \Omega_{02}=a_\odot+\sin^{-1}(-\mathrm{tg}\,i\,\mathrm{tg}\,\delta_\odot)-180° \end{array}\right\} \qquad (i\leqslant 90°-|\delta_\odot|) \qquad (8A)$$

or

$$\left.\begin{array}{l} \Omega_{01}=a_\odot-\sin^{-1}(-\mathrm{ctg}\,i\,\mathrm{ctg}\,\delta_\odot) \\ \Omega_{02}=a_\odot+\sin^{-1}(-\mathrm{ctg}\,i\,\mathrm{ctg}\,\delta_\odot)-180° \end{array}\right\} \qquad (i\geqslant 90°-|\delta_\odot|) \qquad (8B)$$

Now we will explain the two situations corresponding to the two solutions.

By substituting the solution given in formula (7A) into formula (3B), we can obtain maximum photographic latitude φ_{max}:

$$\mathrm{tg}\,\varphi_{max}=\pm\mathrm{tg}\,i$$

At this time, the corresponding photographic latitude range is: φ [i,-i]. This type of situation corresponds to the situation

49

wherein the inclination of the orbit surface is smaller than the inclination of the shadowed great circle surface. At this time, the nodes of the two great circles fall on the apex areas of the orbit's great circle (i.e. the highest and lowest latitude areas of the orbit's great circle).

By substituting the solution given in formula (7B) into formula (3B), we can obtain maximum photographic latitude φ_{max}:

$$\mathrm{tg}\,\varphi_{max} = \pm\mathrm{ctg}\,\delta_\odot$$

The corresponding photographic latitude range is:

$$\varphi\,[i,\ -90° + \delta_\odot]\qquad \delta_\odot > 0$$
$$\varphi\,[90° + \delta_\odot,\ -i]\qquad \delta_\odot < 0$$

This type of situation corresponds to the situation wherein the inclination of the satellite's orbit surface is larger than the inclination of the shadowed great circle surface. At this time, the nodes of the two great circles fall on the apex areas of the shadowed great circle (i.e. the highest and lowest latitude areas of the orbit's great circle).

The following deductions will obtain the maximum photographic area and the proper injection time of the satellite.

We can see from formula (5B) that when the launch date, orbit insertion direction and orbit insertion point of the satellite are given, Ω_o is determined by injection time t_z. Therefore, by properly selecting the injection time (or corresponding launch time) we can cause Ω_o to possess our desired value. For example, by causing Ω_o to satisfy formula (8A) or formula (8B), we can obtain the injection time corresponding to the maximum photographic area:

$$\left.\begin{array}{l} t_{z1} = 12^h + \mathrm{tg}^{-1}(\mathrm{tg}\,\psi\,\sin\varphi_z) - \sin^{-1}(-\mathrm{tg}\,i\,\mathrm{tg}\,\delta_\odot) \\[4pt] t_{z2} = \mathrm{tg}^{-1}(\mathrm{tg}\,\psi\,\sin\varphi_z) + \sin^{-1}(-\mathrm{tg}\,i\,\mathrm{tg}\,\delta_\odot) \end{array}\right\} \quad (i \leqslant 90° - |\delta_\odot|) \qquad (9A)$$

50

or

$$t_{z1} = 12^h + tg^{-1}(tg\,\psi\,\sin\varphi_r) - \sin^{-1}(-ctg\,i\,ctg\,\delta_\oplus)$$
$$t_{z2} = tg^{-1}(tg\,\psi\,\sin\varphi_r) + \sin^{-1}(-ctg\,i\,ctg\,\delta_\oplus)$$
$$\left.\right\} \quad (i \geqslant 90^\circ - |\delta_\oplus|) \qquad (9B)$$

2. The Situation of Observation Satellites With Mission of Photograph in Long Flights

At present, the flight times of observation satellites with missions of photograph can be lengthened to several weeks to several months. This type of satellite generally travels on a sun-synchronous orbit. By appropriately selecting the launch date and launch time, the satellite's photographic area can approach global coverage.

As regards the sun-synchronous orbit, $a_\odot - \Omega$ in formula (3B) can be considered to be constant. It is predetermined by the satellite's flight life, solar light irradiation conditions of the photographic area, the satellite's temperature control and other requirements. By letting $a_\odot - \Omega = \gamma$, seeking the derivative of $tg\,\varphi$ for $\delta_\odot$ and letting its derivative be zero, we can obtain:

$$tg\,\delta_\odot = -\frac{\sin\gamma}{tg\,i} \qquad (10A)$$

The sun's right ascension $a_\odot$ and declination $\delta_\odot$ have the following relational formula:

$$\sin a_\odot = \frac{tg\,\delta_\odot}{tg\,\varepsilon} \qquad (10B)$$

In the formula, ε is the included angle of the ecliptic surface and the earth's equatorial surface. Therefore, it corresponds to obtaining the launch date of the maximum photographic latitude. We can find Ω_0 of the corresponding injection time from the following formula and after substituting it into formula (5B) we can obtain:

$$\Omega_0 = \sin^{-1}\left(\frac{-\sin\gamma}{tg\,i\,tg}\right) - \gamma \qquad (11)$$

By substituting formula (10A) into formula (3B), we can

obtain maximum photographic latitude φ_{max}.

$$\operatorname{tg} \varphi_{max} = \pm \operatorname{tg} i$$

Because sun-synchronous orbit $i > 90°$, the corresponding photographic latitude range is: $\varphi [180°-i, i-180°]$.

VII. The Relationship Between Solar Altitude and Local Time

When satellites with mission of visible photograph take pictures of earth surface targets, it is sometimes necessary to take the pictures at specific solar altitudes (the altitude of the sun from the horizon is the elevation angle). Therefore, it is necessary to know the relationship between the solar altitude and local time.

If the latitude of target area M is φ_M, the altitude of sun S is θ as shown in Fig. 4.
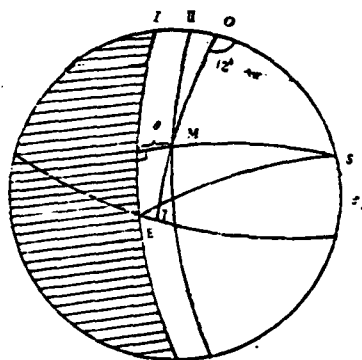

Fig. 4

By passing the M point and making a declination circle, we can obtain spherical surface triangle MOS. From this spherical surface triangle we can obtain:

$$\sin \theta = \sin \delta_\odot \sin \varphi_M - \cos \delta_\odot \cos \varphi_M \cos t_M \qquad (12)$$

The above formula gives the relationship between solar altitude θ and local time t_M.

52

VIII. Numerical Examples

Example 1. A certain known satellite's orbit insertion point latitude $\varphi_z = 35°$ and its orbit entering direction $\gamma = 37°$. We attempt to determine the injection time and cause the ground area which can be photographed by the satellite to be maximum.

Based on the orbit insertion point and orbit insertion direction of the satellite, we can find inclination i of the satellite's orbit surface by the following formula:

$$\cos i = \sin \gamma \cos \varphi_z$$

By substituting the data of the satellite's orbit insertion point latitude and orbit insertion direction into the above formula, we can obtain:

$$i = 60.4°$$

Therefore, we can obtain the two injection times from formula (9A):

$$t_{z1} = 13.5^h - \sin^{-1}(-1.76 \, tg \, \delta_\odot)$$
$$t_{z2} = 1.5^h - \sin^{-1}(-1.76 \, tg \, \delta_\odot)$$

In the above formula, t_{z1} and t_{z2} change with the launch date as shown in Fig. 5.
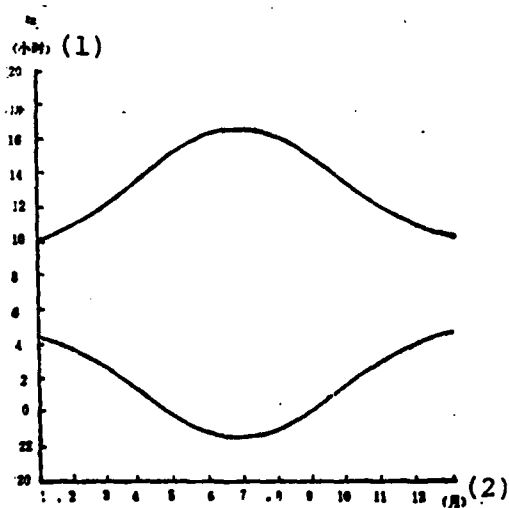

Fig. 5.
Key: (1) Hours; (2) Months.

We can see from Fig. 5 that this satellite can obtain two injection times corresponding to the maximum photographic area: one is daytime and the other is night.

Example 2. It is necessary that the satellite mentioned in the above example photograph a certain focal target and the latitude of this target be 56° north. It is also necessary that the local time for photographing this target area be 10 A.M. and that we try to determine the injection time of the satellite.

By eliminating $\Delta\Omega$ we can obtain the injection time from formula (6):

$$t_z = 7.6^h$$

which is 7:36 A.M.

IX. Discussion

1. The launch time of the satellite, aside from the illumination conditions of the subsatellite point, is usually also limited by many other factors. For example, the requirements of the altitude control system, the solar cell system and the temperature control system etc. Therefore, the launch time of the satellite always requires compromise determination after integrating the requirements of many areas. However, this type of compromise consideration should be established on the basis of the detailed theoretical analysis of each area.

2. If the satellite is required to photograph specific areas at a given local time or at a given solar altitude, at this time we can calculate the injection time of the satellite (example 2) from formula (6). However, for this reason the calculated injection time is the only necessary condition for photographing specific areas in a given time but it is not the full condition. In order to cause the satellite to pass just above the specific area at a given time, it is also necessary to appropriately

54

regulate the orbital period of the satellite.

We would like to express special thanks to comrade Fan Qinhong for his reading, revising and valuable opinions of this article.

References

[1] Wang Jiahe, The Theory of the Operation of Man-Made Satellites, Scientific Publications, 1959.

[2] David R. Brooks, "An Introduction to Orbit Dynamics and Its Application to Satellite-Based Earth Monitoring Missions" NASA RP-1009, November 1977.

SOCIETY DEVELOPMENTS

The Dynamic Environment Conditions Symposium Convenes in Dalian

The "Structural Strength and Environmental Engineering"
Special Committee of the China Aerospace Society convened the
"Dynamic Environment Conditions Symposium" in Dalian on August 17,
1981. 53 representatives from 23 units participated in the con-
ference and 19 technical reports were exchanged. The conference
was chaired by special committee chairman Zhang Jingrong.

The professional participants joined together to summarize
China's experience in dynamic environment engineering of carriers
and satellites, analyze the present situation and find certain
existing problems influencing the development of environmental
engineering such as: 1. the knowledge of vibration sources is not
uniform nor are data processing and the analysis methods; 2.
there is little effective telemetering data and ground measurement
data which has caused blindness in conditions formulation work;
3. the systems level test conditions are deficient; 4. not
enough attention has been given to fundamental research. After
serious discussions and exchanges, they clarified certain long-
standing vague ideas and brought forth seven proposals for
improving environmental conditions work. There was especially
unified understanding of the recent pressing need to develop work
and they proposed: 1. to actively prepare to formulate dynamic
environmental standards for carriers and satellites; 2. to inte-
grate the development of new models to carry out research of
environmental control; 3. five proposals to develop reliable
research to integrate with environmental engineering and research
on the basic theories of environmental engineering.

The environmental conditions work on spacecraft directly
influences its performance and flight reliability. The partici-
pants at the conference unanimously considered that each level of
leadership should give full attention to this work and all at the

56

conference passed the "certain major problems and proposals in formulating spacecraft dynamic environment and test conditions."

The conference triumphantly concluded on August 22 and Li Shuou delivered the closing speech. He said that environmental conditions work was started from scratch, that great achievements were gained and that now was the time for summarizing experiences. He hoped that on the basis of this conference comrades would further summarize experiences and write articles in each field of specialization..... He especially pointed out that the formulation work of environmental conditions was the central link in environmental work. He hoped that everyone would draw on collective wisdom and absorb all useful ideas and as quickly as possible formulate feasible standards. He also said that we must strengthen research work on the environment, replenish the technical contingency, increase necessary equipment, handle well preparatory work and make deserved contributions to research on new products.

The Astronautic New Welding Techniques Exchange Meeting Convenes in Qingdao

The Materials Technology Special Committee and the Spacecraft Manufacturing Technology Committee of the China Aerospace Society jointly sponsored the first "Astronautic New Welding Techniques Exchange Meeting" in Qingdao from August 21 to 25 of 1981. Altogether 69 representatives from 27 units participated in the meeting.

The aim of this meeting was to summarize and exchange experiences for the development of models by welding techniques, exchange results, have mutual study and promote the development of astronautical welding techniques.

The meeting issued a total of 40 articles and technical reports. The major contents of these articles and technical

reports included: materials welding performance; astronautical structural parts welding; braze welding; new technical equipment for welding; special welding as well as welding quality control etc. For example: all of the articles showed that many of the units had done a great deal of work on the welding of new materials such as high strength aluminum alloys, ultra-high-strength steel, martensitic rust-proof steel, heat resisting alloys, integrated product structures to resolve the many technical problems of product welding as well as braze welding techniques, new technical equipment for welding and welding quality control and analysis. There was also a large amount of work done in the area of special welding techniques. The participants at the meeting considered that after exchange, there were gains, raising of standards and predetermined goals were reached.

The meeting also invited Tian Yitang and Wu Lin of Harbin Engineering University, He Fangdian of Qinghua University, Liu Yisheng of Harbin Welding Institute etc. to present reports on welding joint fracture toughness, the use of microprocessors in welding as well as automatic control in the welding process. These reports will have very good guiding effects for future work. The meeting considered that in order to raise astronautical welding quality and raise the reliability of welded components, we should carry out further work in the areas of welding cracks, welding fracture toughness and automatic control in the welding process.

The meeting also held discussions on how to hold specialized academic meetings as well as how to chose academic papers. They also proposed certain beneficial recommendations. Moreover, it was decided that the "Selection of Papers on New Welding Techniques in Astronautics" would be published in the future.

The Special Committee on Measurements and Tests of the China Aerospace Society is Established

The Special Committee on Measurements and Tests of the China Astronautical Society convened an inaugural meeting and its first academic exchange meeting in Beijing from September 3 to 8 of 1981. Participating at the meeting were 88 representatives from 40 units of the National Defense Science Committee System, the Chinese Academy of Sciences, the Chinese Scientific Research Institute of Measurements, institutions of higher learning, the various ministries of machine building etc.

This meeting received a total of 42 papers and reports. Committee Chairman Qiao Shijing presented a report entitled "The Place and Effects of Measurements and Tests in the Aerospace Industry." At the meeting, representatives separately presented reports on "The Important Effects of Measurements and Tests in Space Test Control Techniques," "Developments in Measurements," "The Use of Lasers in Measurements," "The Automation of Measurements and Tests," "Error Analysis" and "Dynamic Parameter Measurements and American Dynamic Test Techniques." These reports caused the representatives to understand the present situation and development techniques of domestic and foreign measurements and tests, broadened their outlooks and clarified their directions.

Aside from these, the five specialized groups of overall planning, long thermodynamics, radio and time frequency separately exchanged papers and reports and there were· rich contents related to each specialized field of measurements and tests of the aerospace system. The main contents were foreign and domestic dynamic states, scientific research results, automatic testing, data processing and error analysis as well as research on measurements and test equipment and precise measuring methods to develop urgently needed products. Pleasing results were attained in studying the close integration of measurements and tests and astronautical scientific research and production and in resolving key problems of products and special measurements and tests. In order to guarantee the precision, quality and reliability of the

aerospace system we brought the important technical foundations and obstructions into play.

In the exchanges, the representatives reviewed the experiences, lessons and achievements in astronautical measurement and test work over the last twenty-five years and fully determined that measurement and test work contributed to China's aerospace industry. In the statements of many of the representatives, it was proposed that measurement and test work should run through the entire process of advance research, test manufacturing, tests, production and use of products. It is one important key in ensuring the quality, reliability and even the success and failure of products. Many of the attending representatives hoped to draw the attention of each level of leadership and related departments because of the instances wherein measurement and test work was unable to keep up which influenced the progress of product research. The representatives said with deep feeling: "Measurement and test work must come before product development." In view of the fact that future demands for measurement and test work will be even higher, the representatives made several recommendations: 1) it was recommended that an assistant designer be in charge of quality and measurement and test work: 2) we must bring forth requirements and formally take on responsibility in the product planning and demonstration stages; 3) we urgently need to reverse the trend of.not checking special testing equipment for a long time, formulate systems and develop work; 4) we must strengthen the departments of measurements and especially build up the basic units of the industry as well as try hard to develop advance research work on measurement and test techniques and fundamental theories.

The meeting also formulated activity plans for each special group for the 1982-1984 period and proposed reliminary ideas for each group to lead the units.

The representatives considered that this meeting was the first

grand meeting of the specialty of astronautical measurements and tests. The astronautical measurement and test techniques possess the special features of using a combination of many branches of learning. This meeting established exchange channels, strengthened connections, had mutual study and relatively large achievements. Because the main object of this meeting was inauguration, time for exchange was short and the number of participants was small. Thus, it could not completely reflect the level of this specialty. It was proposed at the meeting that in the future special groups should be central in carrying out activities and there should be full participation by those in the same field.

As regards the future work of measurements and tests and the special committee, the representatives at the meeting stressed that in order to adapt to the demands for new products with high precision and technical indices, measurements and tests must use various new techniques and develop in the directions of automation, wide frequency bands, wide ranges, many functions, dynamic tests etc.; strengthen basic theoretical research work; strengthen the training of measurement personnel; strengthen the integration of measurement and testing with the products; handle well the journal "Measurement and Test Techniques in Astronautics" and strive to make larger contributions to the development of China's measurement and testing industry.

Standards for Soliciting Contributions for the "Journal of Astronautics

A. The Journal of Astronautics is a comprehensive scientific journal directed by the China Aerospace Society. It uses Marxism and the thought of Mao Zedong as the guiding principles, reflects China's achievements in aerospace science and technology, promotes domestic and foreign scientific exchange and undertakes to realize the four modernizations.

B. The Journal of Astronautics is a quarterly journal

61

distributed domestically and abroad. The readers are mainly
those engaged in scientific research in the aerospace industry,
engineers and technicians, teachers at universities, special-
ized schools and institutes and high level students at those
institutions.

C. The contents of the journal are mainly concerned with the
theories of space flight, astronavigational engineering, techni-
ques (such as spacecraft, power devices, control systems, launch
installations testing instruments etc.), space physics, aero-
space medicine, space biology and space law. It includes:

1. Certain academic reports in theory, practice or the two
combined.

2. Technical reports concerning achievements and advancements
in development and practice as well as those which reflect pre-
sent advanced levels.

3. Comprehensive reviews of certain theories or techniques.

4. Reports and comments on domestic and foreign aerospace
science trends.

D. Requirements for Contributed Articles

1. The thesis must be clear, the writing concise, the data
reliable and the charts and tables clear; scientific articles
are limited to 10,000 characters and technical reports must not
exceed 5,000 characters; the beginning of the article must have
an abstract of the contents (limited to 300 characters) and an
English translation of it, the author's name must be written in
Chinese pinyin romanization and the translation and Chinese
pinyin romanization must be written in block letters.

2. There should be one original and two copies of the contrib-
uted article and the final copy should be a clean copy according
to the requirements of public publishing; it should be written

with a pen on one side of squared paper and each character and
punctuation mark must occupy one square; the writing must be
clear, script characters are not allowed and simplified charact-
ers are to be used.

3. Please write the letters inside and outside the manu-
script in block letters: where italics are necessary, these can
be written in script. When there are different types of writing,
please write notes clearly on the side in pencil for alphabetic
letters which are easily confused or those with sizes which are
not easily distinguished; the position and height of upper and
lower corner letters and numbers on arithmetic symbols must be
clearly distinguished.

4. The charts inserted in the article should accord with
charting standards, use prepared Chinese ink to draw on transpar-
ent or charting paper and it is best for the size of the paper to
be double that used by the journal; the writing in the charts
should be done in pencil, the position of the chart in the manu-
script should be marked by a square and the number of the chart
and its title should be given below the square; photographs of
objects must be sharply demarcated in black and white and be clear;
the charts and photographs should be separately appended and not
pasted on the square paper.

5. The references appended at the end of the paper should be
from well known domestic and foreign books, journals and articles
and it is requested that unpublished material not be used. The
writing form is: number, author's name, name of journal, the date,
volume and number, the page number and the year.

6. It is requested that the real name, work unit, address and
telephone be given: please do not submit a manuscript many times
and do not submit articles which have already been published (with
the exception of restricted publications) for reprinting; for

63

articles published, remunerations will be given according to national stipulations; the editorial department is responsible for returning manuscripts which have not been published.

7. Send contributed articles to: P.O.Box 838, Editorial Department of the China Aerospace Society, Peking.

Notice of Address Change of the China Aerospace Society

Starting January 1, 1982, the China Aerospace Society will have its office at a new address.

Address: No. 2 Beixiao St.,
           Juwai Yuetan, Beijing

Communications: P.O.Box 838, Beijing

Telephone: 89-4602
           89-0651   ext. 303 (office)
                     ext. 450 (editorial office)

Cable address: CSAPK

The original P.O.Box 848 and telephone 89-5040 will be specially used by the China Aerospace Society for outside liaison departments.

DISTRIBUTION LIST

DISTRIBUTION DIRECT TO RECIPIENT

ORGANIZATION	MICROFICHE
A205 DMAHTC	1
A210 DMAAC	1
B344 DIA/RTS-2C	9
C043 USAMIIA	1
C500 TRADOC	1
C509 BALLISTIC RES LAB	1
C510 R&T LABS/AVRADCOM	1
C513 ARRADCOM	1
C535 AVRADCOM/TSARCOM	1
C539 TRASANA	1
C591 FSTC	4
C619 MIA REDSTONE	1
D008 NISC	1
E053 HQ USAF/INET	1
E403 AFSC/INA	1
E404 AEDC/DOF	1
E408 AFWL	1
E410 AD/IND	1
E429 SD/IND	1
P005 DOE/ISA/DDI	1
P050 CIA/OCR/ADD/SD	2
AFIT/LDE	1
FTD	
CCN	1
NIA/PHS	1
NIIS	2
LLNL/Code L-389	1
NASA/NST-44	1
NSA/1213/TDL	2

DATE
ILME